

AIR FORCE REPORT NO.  
SAMSO-TR-73-136

328  
AEROSPACE REPORT NO.  
TR-0073 (3450-16) -2

A73  
01458

C1

5026242

# Predicted Radar Cross Section of Thin, Long Wires Compared with Experimental Data

Prepared by J. RENAU and M. T. TAVIS  
Electronics and Optics Division  
Engineering Science Operations

72 OCT 01

DO NOT DESTROY  
RETURN TO LIBRARY

---

Reentry Systems Division  
THE AEROSPACE CORPORATION

---

Prepared for SPACE AND MISSILE SYSTEMS ORGANIZATION  
AIR FORCE SYSTEMS COMMAND  
LOS ANGELES AIR FORCE STATION  
Los Angeles, California

PROPERTY OF  
AEROSPACE CORPORATION

APR 1 6 1973

APPROVED FOR PUBLIC RELEASE: DISTRIBUTION RETURN TO LIBRARY

Air Force Report No.  
~~2~~ SAMSO-TR-73-136

Aerospace Report No.  
TR-0073(3450-16)-2

PREDICTED RADAR CROSS SECTION OF THIN, LONG WIRES  
COMPARED WITH EXPERIMENTAL DATA

Prepared by  
J. Renau and M. T. Tavis

Radar and Power Subdivision  
Electronics and Optics Division  
Engineering Science Operations

72 OCT 01

Reentry Systems Division  
THE AEROSPACE CORPORATION  
El Segundo, California

Prepared for  
SPACE AND MISSILE SYSTEMS ORGANIZATION  
~~2~~ AIR FORCE SYSTEMS COMMAND  
LOS ANGELES AIR FORCE STATION  
Los Angeles, California

Approved for public release;  
distribution unlimited

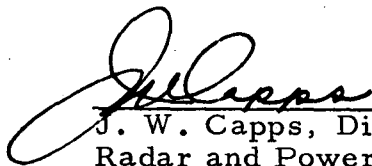
## FOREWORD

This report is published by The Aerospace Corporation, El Segundo, California, under Air Force Contract No. F04701-72-C-0073. This report was prepared by the Electronics and Optics Division, Engineering Science Operations, at the request of Concepts and Plans Group, Reentry Systems Division.

This report, which documents research carried out from December 1971 through September 1972, was submitted for review and approval on 31 January 1973 to Ronald L. Adams, 2nd Lt, USAF, SAMSO (RSSG).

The authors acknowledge with gratitude the assistance of Mary Barling, John Kohlenberger and Dr. William Helliwell who aided in preparing the computer-generated figures used in this study. The authors also thank Dr. Duclos for his backing of the study.

Approved by



J. W. Capps, Director  
Radar and Power Subdivision  
Electronics and Optics Division  
Engineering Science Operations



---

G. R. Schneiter, Director  
Program Definition  
Concepts and Plans  
Reentry Systems Division  
Development Operations

Publication of this report does not constitute Air Force approval of the report's findings or conclusions. It is published only for the exchange and stimulation of ideas.



---

Ronald L. Adams, 2nd Lt, USAF  
ECM/Pen Aids Project Officer  
System Engineering Directorate  
Deputy for Reentry Systems

## ABSTRACT

In order to determine the validity and accuracy of Radar Cross Section (RCS) predictions for thin wires, the predictions of the closed-form expressions developed by Chu, Tai, Van Vleck, et al., and Ufimtsev have been compared with carefully measured backscattered RCS vs angle of incidence for various length thin, long, cylindrical conductors. Further, the prediction of an open-form numerical analysis based on the Source Distribution Technique and programmed by M. B. Associates as the BRACT computer program was also compared with the experimental data.

It was found that (1) the BRACT computer results agree with experiment so well (within  $\pm 1$  dB for all reliable data) that it may be used with great confidence for any length thin wires and can be used as reference data for comparing with the predictions of the closed-form solutions; (2) the results of Chu are not accurate except at broadside incidence; (3) the results of Tai compare favorably with data up to  $k\ell$  values of about 17 if corrections are made to the approximate formulas to correct for broadside incidence; (4) the results of Ufimtsev compare well with experiment for all  $k\ell$  values considered; and (5) the results of Van Vleck, et al., appear to be very accurate for all  $k\ell$  values considered except for near end-on incidence. In a separate report to be published soon one of the authors of this report (M. Tavis) has shown that this deficiency is due to numerical approximations in the theoretical expressions.

## CONTENTS

ABSTRACT . . . . .	iii
I. INTRODUCTION . . . . .	1
II. WIRE DIMENSIONS AND RCS DATA . . . . .	3
III. THEORETICAL EXPRESSIONS AND THE SDT COMPUTER PROGRAM . . . . .	5
A. A Review of Tai's Theoretical Expressions and Comparison of Predictions with Data . . . . .	7
B. Predictions Based on Van Vleck's, et al., Expression and Comparison with Data . . . . .	10
C. Ufimtsev's Solution . . . . .	12
D. SDI Technique . . . . .	15
IV. CONCLUSIONS . . . . .	17
REFERENCES . . . . .	19
APPENDIX A . . . . .	A-1

## FIGURES

1.	Measured Backscattered RCS for Thin, Metallic Straight Wires, $kl = 4.44$ , Circular Polarization . . . . .	21
2.	Measured Backscattered RCS for Thin, Metallic Straight Wires, $kl = 9.2$ , Circular Polarization . . . . .	22
3.	Measured Backscattered RCS for Thin, Metallic Straight Wires, $kl = 11.7$ , Linear Polarization . . . . .	23
4.	Measured Backscattered RCS for Thin, Metallic Straight Wires, $kl = 13$ , Circular Polarization . . . . .	24
5.	Measured Backscattered RCS for Thin, Metallic Straight Wires, $kl = 17$ , Linear Polarization . . . . .	25
6.	Measured Backscattered RCS for Thin, Metallic Straight Wires, $kl = 34.8$ , Linear Polarization . . . . .	26
7.	Measured Backscattered RCS for Thin, Metallic Straight Wires, $kl = 45.7$ . . . . .	27
8.	Comparison of Tai's Predicted RCS with Measured Data, $kl = 11.7$ . . . . .	28
9.	Comparison of Chu's Predicted RCS with Measured Data, $kl = 11.7$ . . . . .	29
10.	Comparison of Tai's Predicted RCS with Measured Data, $kl = 4.44$ . . . . .	30
11.	Comparison of Chu's Predicted RCS with Measured Data, $kl = 4.44$ . . . . .	31
12.	Comparison of Modified Tai's Prediction with Measured RCS Data, $kl = 11.7$ . . . . .	32
13.	Comparison of Modified Tai's Prediction with Measured RCS Data, $kl = 13$ . . . . .	33
14.	Comparison of Modified Tai's Prediction with Measured RCS Data, $kl = 9.2$ . . . . .	34

FIGURES (cont.)

15.	Comparison of Modified Tai's Prediction with Measured RCS Data, $kl = 4.44$ . . . . .	35
16.	Comparison of Modified Tai's Prediction with Measured RCS Data, $kl = 17$ . . . . .	36
17.	Comparison of Modified Tai's Prediction with Measured RCS Data, $kl = 45.7$ . . . . .	37
18.	Comparison of Van Vleck's Predicted RCS with Measured Data, $kl = 4.44$ . . . . .	38
19.	Comparison of Van Vleck's Predicted RCS with Measured Data, $kl = 9.2$ . . . . .	39
20.	Comparison of Van Vleck's Predicted RCS with Measured Data, $kl = 11.7$ . . . . .	40
21.	Comparison of Van Vleck's Predicted RCS with Measured Data, $kl = 13$ . . . . .	41
22.	Comparison of Van Vleck's Predicted RCS with Measured Data, $kl = 17$ . . . . .	42
23.	Comparison of Van Vleck's Predicted RCS with Measured Data, $kl = 45.2$ . . . . .	43
24.	Comparison of Ufimtsev's Predicted RCS with Measured Data, $kl = 4.44$ . . . . .	44
25.	Comparison of Ufimtsev's Predicted RCS with Measured Data, $kl = 9.2$ . . . . .	45
26.	Comparison of Ufimtsev's Predicted RCS with Measured Data, $kl = 11.7$ . . . . .	46
27.	Comparison of Ufimtsev's Predicted RCS with Measured Data, $kl = 13$ . . . . .	47
28.	Comparison of Ufimtsev's Predicted RCS with Measured Data, $kl = 17$ . . . . .	48

## FIGURES (cont.)

29. Comparison of Ufimtsev's Predicted RCS with Measured Data, $k\ell = 45.7$ . . . . .	49
30. Comparison of BRACT Calculated RCS with Measured Data, $k\ell = 4.44$ . . . . .	50
31. Comparison of BRACT Calculated RCS with Measured Data, $k\ell = 9.2$ . . . . .	51
32. Comparison of BRACT Calculated RCS with Measured Data, $k\ell = 11.7$ . . . . .	52
33. Comparison of BRACT Calculated RCS with Measured Data, $k\ell = 13$ . . . . .	53
34. Comparison of BRACT Calculated RCS with Measured Data, $k\ell = 17$ . . . . .	54
35. Comparison of BRACT Calculated RCS with Measured Data, $k\ell = 34.8$ . . . . .	55
36. Comparison of BRACT Calculated RCS with Measured Data, $k\ell = 45.7$ . . . . .	56
37. BRACT Calculated RCS, $k\ell = 157$ . . . . .	57
38. Van Vleck vs Ufimtsev Predicted RCS Values, $k\ell = 157$ . . . . .	59
39. Comparison of the Generalized Van Vleck Formulation with Van Vleck's original Expression, $k\ell = 13$ . . . . .	61

## TABLE

1. Experiment Parameters . . . . .	4
------------------------------------	---

## I. INTRODUCTION

Interest in the backscattered Radar Cross Section (RCS) of thin, long, cylindrical conductors has led several organizations including The Aerospace Corporation to obtain RCS measurements vs angle of incidence for various length thin, long, conducting wires.

Having assembled such carefully measured RCS data, it was logical to use the more commonly known closed-form theoretical expressions published in the literature on this subject for comparison purposes. The relatively simple analytical expressions used are those derived by Chu (unpublished but discussed by Van Vleck, et al., in Ref. 1, and used in Ref. 2), by Van Vleck, et al. (Ref. 1), and Tai (Ref. 3),\* and the known expressions derived by Ufimtsev in relatively recent publications (Refs. 4 and 5).

The purpose of this technical report is twofold. The first purpose is to compare the predictions from the four theoretical expressions with the data over a wide range of length-to-wavelength ratios in order to establish which theoretical expression possesses general validity for predicting all the experimental data considered and to within what accuracy. The second purpose is to compare with the data the RCS predictions obtained by using a computer program specifically designed to yield the RCS of thin, not necessarily straight, conducting wires.

---

\*Equations (21) and (22) given by Tai are expressions averaged over the polarization angle. In order to recover the expression before the averaging process, multiply Eqs. (21) and (22) of Tai by  $8/3 \cos^4\psi$ . Moreover, there is a misplaced bracket in the logarithmic term of these equations. For this reason, the corrected forms will be given in the text of this report.

## II. WIRE DIMENSIONS AND RCS DATA

In May 1968, an RCS experiment on thin wire configurations was conducted at the Radar Target Scatter (RATSCAT) Division at Holloman Air Force Base, New Mexico. This experiment was directed by J. W. Curtis and L. Martinez of The Aerospace Corporation. A thin, straight wire was one of the configurations measured under this effort. The radar frequency chosen for the straight wire experiment was 450 MHz (radar wavelength  $\lambda = 2/3$  m). Because of practical limitations, yet desiring to achieve a large value of  $k\ell$  (where  $k\ell = 2\pi\ell/\lambda$  and  $2\ell = L$  = total length of wire), a copper wire with a total length of 2.48 m was chosen, i.e.,  $k\ell = 11.7$ . The radius of the wire was "a" =  $4 \times 10^{-4}$  m (15.8 mil) or  $ka = 2\pi a/\lambda = 3.78 \times 10^{-3}$ . The linearly polarized electric field vector of the radar was chosen in the plane formed by  $\vec{k}$  and  $\vec{l}$  so that  $\cos \psi = 1$ . The wire located in the far field of the radar was mounted on a very low RCS support (styrofoam holder) such that -40 dbsm cross section could be measured with a signal-to-noise ratio of about 10 dB. The calibration measurements performed on known size spheres were accurate to within 1 dB of the predicted RCS. During the RCS vs angle measurement, the angular accuracy was about  $\pm 1$  deg. Subsequently, the measured RCS values of more pieces of differing length wires became available, and the seven almost randomly selected data for presentation in this report are a good representation of reliable RCS measurements over a wide range of  $k\ell$  values, where the radius "a" of each wire is such that  $ka \ll 1$ .

The measured backscattered RCS data in decibels relative to a meter square (dbsm) vs aspect angle (90 deg at broadside) for the differing length, thin, metallic straight wires are shown in Figs. 1 through 7.\* The accuracy of the RCS measurements is within about 3 dB at the peaks and degrades at the

---

\* In Fig. 7, the angle  $\theta$  is zero at broadside and 90 deg at grazing incidence.

nulls of the RCS patterns based on calibrating spheres. The errors in the Avco data (Fig. 6) are larger. The angular accuracy is about  $\pm 1$  deg. The pertinent parameters of each experiment are given in Table 1.

Table 1. Experiment Parameters

Fig. No.	Source of Data	Wavelength, m	Polarization <sup>a</sup>		ka	$kl$
			Transmit	Receive		
1	Lincoln Lab. (Ref. 6), per- formed by Sigma Inc., Fla.	0.227	Circular	Circular	$4.2 \times 10^{-3}$	4.44
2	Lincoln Lab (Ref. 6)	0.227	Circular	Circular	$4.2 \times 10^{-3}$	9.2
3	SAMSO/ Aerospace Corp., per- formed at RATSCAT	0.666	Linear	Linear	$3.78 \times 10^{-3}$	11.7
4	Lincoln Lab <sup>b</sup> (Ref. 6)	0.227	Circular	Circular	$4.2 \times 10^{-3}$	13
5	Univ. Michigan	Set at 1.00	Linear	Linear	$3.95 \times 10^{-2}$	17
6	Avco <sup>c</sup>	0.69	Linear	Linear	$9.1 \times 10^{-3}$	34.8
7	M. B. Assoc- iates, per- formed at Sigma Inc., Fla.	Set at 1.00	Linear	Linear	0.22	45.7

<sup>a</sup>Circular Transmit and Receive RCS will be 6 dB below that of Linear Transmit and Receive.

<sup>b</sup>Lincoln Labs data appears to be somewhat in error up to the first null.

<sup>c</sup>Avco data is several decibels in error due to experimental difficulties.

### III. THEORETICAL EXPRESSIONS AND THE SDT COMPUTER PROGRAM

Tai's expression (Ref. 3, Eq. 21) for the backscattered RCS from long thin wires with  $k\ell \gg 1$  and  $ka \ll 1$  when the wire is nonresonant (namely  $k\ell$  is not equal to  $\frac{n\pi}{2}$ ,  $n = 1, 2, 3, \dots$ ) is

$$\begin{aligned} \frac{\sigma}{\lambda^2} &= \frac{1}{\pi} \frac{P(\psi)}{\left(\frac{\pi}{2}\right)^2 + \left[\ln\left(\frac{\gamma k a \sin\theta}{2}\right)\right]^2} \\ &\times \frac{1}{\sin^4\theta} \left[ \frac{1 + \cos^2\theta}{2\cos\theta} \sin(2k\ell\cos\theta) \right. \\ &\quad \left. - \frac{1 - \cos(2k\ell)\cos(2k\ell\cos\theta)}{\sin 2k\ell} \right]^2 \end{aligned} \quad (1)$$

The expression derived by Chu (unpublished) for the same conditions and referenced by Van Vleck, et al. (Ref. 1), also given in Ref. 2, is

$$\frac{\sigma}{\lambda^2} = \frac{1}{\pi} \frac{P(\psi)}{\left(\frac{\pi}{2}\right)^2 + \left[\ln\left(\frac{\gamma k a \sin\theta}{2}\right)\right]^2} \sin^2\theta \left[ \frac{\sin(2k\ell\cos\theta)}{2\cos\theta} \right]^2 \quad (2)$$

where

$\sigma$  = radar cross section

$a$  = radius of wire

$2\ell$  = total length of wire

$\ln x$  = natural logarithm of  $x$

$\ln \gamma$  = 0.5772 or  $\gamma \approx 1.78$

$k = \frac{2\pi}{\lambda}$

$\theta$  = aspect angle ( $\theta = 90$  deg at broadside incidence)

$\psi$  = polarization angle, defined as the acute angle between the incident electric field vector and the plane defined by  $\vec{k}$  and  $\vec{l}$

$P(\psi) = \cos^4 \psi$  for the case of transmitted linearly polarized waves and received in the same direction; for random polarization,

$$\overline{P} = \frac{1}{2\pi} \int_0^{2\pi} \cos^4 \psi d\psi = \frac{3}{8}.$$

$P(\psi) = \frac{\cos^2 \psi}{2}$  transmit linear, receive right or left circular

$P(\psi) = \frac{1}{4}$  transmit right or left circular, receive right or left circular

To test the validity of the theoretical expressions for thin, long wires of infinite conductivity, the parameters of the copper wire used at the RATSCAT Center were inserted in the expressions Eqs. (1) and (2), with  $P(\psi) = 1$ , and the predicted cross sections  $\sigma(\theta)$  vs  $\theta$  were obtained. The predictions from Tai's expression are plotted in Fig. 8, where the experimental data are also shown for comparison. The predictions obtained from Chu's expression, together with the same data, are plotted in Fig. 9. In both figures, the ordinate is the absolute backscattered cross section in dbsm vs the aspect angle with respect to the wire.

The results of Figs. 8 and 9 indicate that for  $kL = 11.7$ , Tai's expression predicts the correct number of lobes in the RCS vs angle pattern and, within a few decibels and degrees in position, the magnitude of the predicted RCS agrees with the data except near the nulls. Chu's expression yields results that agree very well with the data only near broadside (aspect angle near 90 deg), but leads to very erroneous results at all other angles. Chu's expression for all the other wires discussed in this report led to similar erroneous results, except at broadside incidence.

A further test of Tai's and Chu's expressions is obtained by using the parameters of Fig. 1 and Table 1. The predicted values from Tai's expression are shown in Fig. 10 and those of Chu's in Fig. 11. In both figures, the data have also been plotted for comparison purposes. It is clear that Chu's expression for broadside is the more accurate one.

A comparison of Eqs. (1) and (2) for the aspect angle  $\theta = 90$  deg reveals that Tai's expression at broadside reduces to:

$$\frac{\sigma}{\lambda^2} = \frac{1}{\pi} \frac{P(\psi)}{\left(\frac{\pi}{2}\right)^2 + \left[\ell \ln\left(\frac{\gamma k a}{2}\right)\right]^2} \left(k\ell - \frac{1 - \cos 2k\ell}{\sin 2k\ell}\right)^2 \quad (3)$$

and Chu's expression reduces to:

$$\frac{\sigma}{\lambda^2} = \frac{1}{\pi} \frac{P(\psi)}{\left(\frac{\pi}{2}\right)^2 + \left[\ell \ln\left(\frac{\gamma k a}{2}\right)\right]^2} (k\ell)^2 \quad (4)$$

Equations (3) and (4) at  $\theta = 90$  deg are identical except for the second term in brackets in Tai's expression. Indeed, it will be shown below that the correct asymptotic ( $k\ell \gg 1$ ) equation that one obtains from Tai's expression at  $\theta = 90$  deg, i.e., broadside, is Eq. (4) and not Eq. (3) as published.

#### A REVIEW OF TAI'S THEORETICAL EXPRESSIONS AND COMPARISON OF PREDICTIONS WITH DATA

According to Ref. 3, Eq. (26), when a linearly polarized wave with the electric field in the plane of incidence is incident broadside ( $\theta = 90$  deg) upon a thin, metallic wire, of infinite conductivity, the radar cross section  $\sigma$  is given by

$$\frac{\sigma}{\lambda^2} = \frac{1}{\pi} \left| \frac{g_o^2}{Y_o} \right|^2 \quad (5)$$

where

$$g_o = 2(\sin x - x \cos x)$$

$$\gamma_o = 2\cos^2 x(-1 + \cos 2x - j \sin 2x) + j 2 \cos x(x \cos x - \sin x)(\ln 4 + \Omega - 2L(2x))$$

$$x = k\ell = \frac{2\pi\ell}{\lambda}, \quad 2\ell = \text{total length of wire}$$

$$\Omega = 2\ell \ln \frac{2\ell}{a}$$

a = radius of wire

$$L(y) \equiv \int_0^y \frac{1 - e^{-ju}}{u} du = \bar{Ci}(y) + j Si(y), \text{ for any variable } y$$

$$Ci(y) \equiv \int_0^y \frac{1 - \cos u}{u} du = \ell \ln(\gamma y) - Ci(y)$$

$$\gamma \approx 1.78$$

$$Si(y) \equiv \int_0^y \frac{\sin u}{u} du$$

$$Ci(y) \approx \frac{\sin y}{y} \text{ for } y \gg 1$$

$$Si(y) \approx \frac{\pi}{2} - \frac{\cos y}{y} \text{ for } y \gg 1$$

Therefore,

$$L(y) \approx \ell \ln(\gamma y) + j \frac{\pi}{2} \text{ for } y \gg 1$$

When  $x \gg 1$  and  $x \neq n\frac{\pi}{2}$  so that  $x\cos x \gg \sin x$ , inserting from the above definitions, and neglecting higher order terms, one finds that

$$\frac{g_o^2}{\gamma_o} \approx \frac{4x^2 \cos^2 x}{2\cos^2 x(-1 + \cos 2x - j\sin 2x) + j2x\cos^2 x(\ln 4 + \Omega - 2\ln 2\gamma x) + 2\pi x\cos^2 x}$$

Since

$$\ln 4 + \Omega - 2\ln 2\gamma x = 2\ln \frac{2}{\gamma k a} = -2\ln \left( \frac{\gamma k a}{2} \right)$$

then

$$\frac{g_o^2}{\gamma_o} \approx \frac{2x}{\pi - j \left[ 2\ln \left( \frac{\gamma k a}{2} \right) \right]} \text{ for } x \gg 1$$

and

$$\frac{\sigma}{\lambda^2} = \frac{1}{\pi} \left| \frac{g_o^2}{\gamma_o} \right|^2 \approx \left( \frac{1}{\pi} \right)^2 \frac{x^2}{\left( \frac{\pi}{2} \right)^2 + \left[ \ln \left( \frac{\gamma k a}{2} \right) \right]^2} = \frac{1}{\pi} \frac{(k\ell)^2}{\left( \frac{\pi}{2} \right)^2 + \left[ \ln \left( \frac{\gamma k a}{2} \right) \right]^2}. \quad (6)$$

Equation (6), derived from Tai's own general expression, is identical, at  $\theta = 90$  deg, to Chu's expression, Eq. (4). At this point it was obvious that the complete general expressions of Tai's derivation should be used rather than the asymptotic expression given by Tai. However, simplicity of his long wire expression is appealing from a practical point of view, since the general expressions are rather lengthly. In order to preserve the simple expression of Tai (Ref. 3, Eq. 21) a simple arbitrary function  $f(\theta)$  is chosen that modifies the second term in brackets of Tai's Eq. (1), and modifies it only near broadside so that, for  $k\ell \gg 1$ , it properly reduces to Eq. (4) or (6). That is

$$f(\theta) = 1 - \left( \frac{\sin(2k\ell \cos \theta)}{2k\ell \cos \theta} \right)^2 \sin^2 \theta, \text{ for } k\ell \gg 1,$$

where  $f(\theta) \approx 1$  for all values of  $\theta$  except for  $\theta \rightarrow 90$  deg, where  $f(\theta) \rightarrow 0$  near broadside. The new expression for the RCS of a non-resonant thin, long, metallic wire may be written as

$$\frac{\sigma}{\lambda^2} = \frac{1}{\pi} \frac{P(\psi)}{\left(\frac{\pi}{2}\right)^2 + \left[\ln\left(\frac{\gamma k a \sin \theta}{2}\right)\right]^2} \times \frac{1}{\sin^4 \theta} \left[ \frac{1 + \cos^2 \theta}{2 \cos \theta} \sin(2k\ell \cos \theta) - f(\theta) \frac{1 - \cos(2k\ell) \cos(2k\ell \cos \theta)}{\sin 2k\ell} \right]^2 \quad (7)$$

Predictions of the RCS based on Tai's modified expression, Eq. (7), for the wires described in Table 1, are shown in Figs. 12 through 17 together with the appropriate data. As can be seen, the modified Tai's expression for the RCS of thin, long, nonresonant, metallic wires predicts the RCS vs aspect angle for  $4.5 < k\ell < 17$  within a few decibel over the entire aspect angle variation, except near the nulls. However, for  $k\ell \geq 45.7$ , the predictions vary by more than 10 dB from the measurements. Since the modified Tai's expressions are simple, they may be used for quick and fairly accurate estimates for the  $k\ell$  values given above.

#### B. PREDICTIONS BASED ON VAN VLECK'S, ET AL., EXPRESSION AND COMPARISON WITH DATA

The expression derived by the above authors (Ref. 1) was one of the earliest in this field. Even though S. Hong (Ref. 4) claims Van Vleck's study to only be applicable to short wires, our experience has been that Van Vleck's expressions are of much greater general validity than given credit. This can be seen in Figs. 18 through 23, which are the predictions obtained when the parameters of the wires of Table 1 were used for the predictions. The

cross section expression of Van Vleck, et al. (Ref. 1), is reproduced here for easy reference. Note that these are Van Vleck's approximate formulas.

$$\sigma = 4\pi P(\Phi) \left| (F' + F'') \frac{\sin 2q\ell}{q} + 2(G' + jG'') \cos(q\ell) \left[ \frac{\sin(q + \beta)\ell}{q + \beta} \right. \right. \\ \left. \left. + \frac{\sin(q - \beta)\ell}{q - \beta} \right] + 2(H' + jH'') \sin(q\ell) \left[ \frac{\sin(q + \beta)\ell}{q + \beta} - \frac{\sin(q - \beta)\ell}{q - \beta} \right] \right|^2 \quad (8)$$

where

$P(\Phi)$  = as given in the text

$$F' = \frac{\Omega'}{(\Omega')^2 + \pi^2}$$

$$F'' = \frac{\pi}{(\Omega')^2 + \pi^2}$$

$$\Omega' = 2 \log_e \frac{\lambda}{\pi a} - 1.154$$

$$2G' = \frac{\psi(\beta\ell)}{\psi^2(\beta\ell) + Z^2(\beta\ell)} - \frac{\pi}{2} \frac{2G''}{\Omega'}$$

$$2G'' = \frac{Z(\beta\ell)}{\psi^2(\beta\ell) + Z^2(\beta\ell)}$$

$$2H' = \frac{\psi(\beta\ell - \pi/2)}{\psi^2(\beta\ell - \pi/2) + Z^2(\beta\ell - \pi/2)} - \frac{\pi}{2} \frac{2H''}{\Omega'}$$

$$2H'' = \frac{Z(\beta\ell - \pi/2)}{\psi^2(\beta\ell - \pi/2) + Z^2(\beta\ell - \pi/2)}$$

$$\psi(y) = -(\Omega' - \Delta) \times \cos y + (\pi/4) \sin y$$

$$Z(y) = (1/2) [\log_e (4\beta\ell) + 0.577] \sin y - (\pi/4) \cos y$$

$$\Delta = -(1/2)[\log_e (\beta l)] + 0.712$$

$$q = \beta \cos \theta$$

$$\beta = 2 \pi / \lambda$$

$\lambda$  = radar wavelength

$2l$  = total length of wire element

$a$  = radius of wire element

$\theta$  = angle between line-of-sight from the radar to the wire element and the axis of the wire element

$$j = \sqrt{-1}$$

As can be seen from Figs. 18 through 23, the expressions used by Van Vleck, et al., when compared with the data, give good RCS results for all the cases shown except for end-on incidence. The difference between data and predictions in all cases is within 4 dB at the peaks and within 2 to 3 deg in look angle. The accuracy in the nulls is not quite as good. Tai and Van Vleck are about equally as accurate at the lower  $kl$  values.

### C. UFIMTSEV'S SOLUTION

The RCS of long, thin wires as given by Ufimtsev (Ref. 5) is taken from Ref. 4 and given below. The predictions based on these equations are compared with data in Figs. 24 through 29.

#### 1. THE CASE FOR $\theta \neq \pi/2$

$$\sigma(\theta, \phi)/\lambda^2 = \frac{4 \cos^4 \phi \cdot |S(\theta)|^2}{\pi \sin^2 \theta \cdot \sin^2(2\theta) \left| \ln\left(\frac{2i}{\gamma k a \sin \theta}\right) \right|^4}$$

where

$$\begin{aligned}
 S(\theta) = & -\sin^4\left(\frac{\theta}{2}\right) \cdot \ln\left[\frac{i}{\gamma ka \sin^2(\theta/2)}\right] \\
 & + e^{ikL2\cos\theta} \cdot \cos^4\left(\frac{\theta}{2}\right) \cdot \ln\left[\frac{i}{\gamma ka \cos^2\left(\frac{\theta}{2}\right)}\right] \\
 & + e^{ikL(1+\cos\theta)} \cdot 2 \cdot \left\{ \sin^4\left(\frac{\theta}{2}\right) \cdot \psi_- \cdot \ln\left[\frac{i}{\gamma ka \sin\left(\frac{\theta}{2}\right)}\right] \right. \\
 & \quad \left. - \cos^4\left(\frac{\theta}{2}\right) \cdot \psi_+ \cdot \ln\left[\frac{i}{\gamma ka \cos\left(\frac{\theta}{2}\right)}\right] \right\} \\
 & + \frac{\cos\theta}{D} \cdot \ln\left(\frac{i}{\gamma ka}\right) \cdot \left[ e^{ikL2} (\psi_+)^2 + e^{ikL2(1+\cos\theta)} (\psi_-)^2 \right. \\
 & \quad \left. - 2 e^{ikL(3+\cos\theta)} \cdot \psi_- \cdot \psi_+ \right]
 \end{aligned}$$

$$\gamma = 1.781$$

$$\psi = \frac{i\pi - 2\ln(\gamma ka)}{\ln\left(\frac{i2kL}{\gamma k^2 a^2}\right) - E(2kL) e^{-i2kL}}$$

$$\psi_{\pm} = \frac{i\pi - \ln(\gamma^2 q_{\pm})}{\ln\left(\frac{i2kL}{\gamma k^2 a^2}\right) - E\left(\frac{2kLq_{\pm}}{k^2 a^2}\right) \cdot e^{-i2q_{\pm} \frac{kL}{k^2 a^2}}}$$

$$q_{\pm} = \frac{(ka)^2}{2} (1 \mp \cos\theta)$$

$$E(y) = \int_{-\infty}^y \frac{\cos t}{t} dt + i \int_0^y \frac{\sin t}{t} dt - i\pi/2$$

$$D = 1 - \psi^2 \cdot e^{i2kL}$$

$a$  = radius of the wire

$L$  = total length of the wire

$\theta$  = the angle between the propagation vector and the wire

$\phi$  = the angle between the  $E$  vector and the wire

## 2. THE CASE FOR $\theta = \pi/2$

$$\sigma(\theta = \pi/2, \phi)/\lambda^2 = \frac{\cos^4 \phi}{\pi} \times |\tilde{S}|^2$$

where

$$\begin{aligned}\tilde{S} &= \frac{ikL}{2A} - ikL \frac{(\bar{\Psi})^2}{2A^2} \frac{E(2kL)}{A^2} + \frac{A - 1/2}{A^2} \\ &\quad + \frac{2}{A^2} \left[ \frac{\bar{\Psi}}{4} - \ln \left( \frac{i\sqrt{2}}{\gamma ka} \right) \right] \bar{\Psi} e^{ikL} \\ &\quad + \frac{2(\bar{\Psi})^2}{DA^2} \times \ln \left( \frac{i}{\gamma ka} \right) (e^{i2kL} - \bar{\Psi} e^{i3kL}) \\ A &= \ln \left( \frac{2i}{\gamma ka} \right) \\ \bar{\Psi} &= \Psi_{\pm} (\theta = \pi/2)\end{aligned}$$

As can be seen from Figs. 24 through 29, Ufimtsev's results compare very well with data for all  $kL$  values considered. However, the expressions are complicated and the modified Tai may be used easily for the smaller  $kL$  values. The location of the peaks and valleys compares well with the data and the accuracy of the predictions is comparable to that predicted by Van Vleck.

#### D. SDI TECHNIQUE

The SDI technique has been used by M. B. Associates to develop a computer program designated as BRACT (Ref. 7). The BRACT program uses the numerical solution of the thin wire integral equation to solve the complete electromagnetic scattering problem for arbitrary wire structures. For these arbitrary scatterers, the program sets up the structure matrix relating the incident field to the resulting induced currents and calculates the induced current distribution on the scatterer. The currents thus obtained are used to calculate the scattered fields. BRACT is designed for execution on the Control Data Computing System and is coded in FORTRAN IV as released under the SCOPE version 3.1.2 operating system.

This program was used to calculate the RCS of long wires, using the data presented in Table 1. The results are compared with experiment in Figs. 30 through 36. As can be seen, the calculated values for all values of  $k\ell$  are nearly on top of the data except for the two cases,  $k\ell = 13$  and  $k\ell = 34.8$  where the differences are about 4 dB. It is known that the data for  $k\ell = 34.8$  is in error, and it is believed that the data for  $k\ell = 13$  is also in error, since every theoretical technique applied gives more error for these two cases than all other cases. BRACT was also used to calculate the RCS of a wire with  $k\ell = 157$ ,  $\lambda = 2$  cm, and a radius of  $1.52 \times 10^{-4}$  m ( $\ll \lambda$ ). The results are presented in Fig. 37.

In order to prove the accuracy of the Ufimtsev and Van Vleck closed-form expressions for very long wires, the RCS of the long wire  $k\ell = 157$  was calculated using the expressions of these authors and the results are given in Fig. 38. The results obtained by BRACT and the results obtained by the closed-form expressions are nearly identical, being about 1 dB different at the peaks and following the dips very closely, although Van Vleck's expression predicts much lower null values than the other two cases.

#### IV. CONCLUSIONS

The comparison of the results of the calculations with measured back-scattered data from various length, thin, cylindrical conductors shows that, of the four analytical expressions, Chu's expression yields fair RCS agreement with the data only at broadside incidence. The modified Tai's predictions at all angles are within a few decibels of the RCS data for wires of  $4.5 < k\ell < 17$ , where  $k\ell = \frac{2\pi\ell}{\lambda}$ ,  $2\ell$  = total length of wire, and  $\lambda$  = wavelength. For larger values of  $k\ell$ , Tai's expression yields predicted values which differ from the data by as much as 10 dB. Van Vleck's expressions lead to predictions that are within a few decibels of the RCS data at all angles greater than 20 deg from end-on, and for all thin wires tested, namely  $k\ell > 4.5$ . Even end-on, the predictions can be used as an estimate if it is noted that the RCS should approach zero as  $\theta \rightarrow 0$ . The predictions from Ufimtsev's analytical expression yield results that are no more accurate than those of Van Vleck (except near end-on incidence) and in the nulls. Except for end-on incidence, Van Vleck's approximate expressions are as good or better than all others if one is willing to let the RCS approach zero at end-on by using the shape of the last lobe in the pattern as a guide. In Ref. 8 it is shown that the deficiency in Van Vleck's theoretical predictions at end-on are associated with approximations as published, and when the general expressions given by Van Vleck are used, the deficiency of the theoretical predictions at end-on disappear. In appendix A these expressions are given and in Fig. 39 a comparison of the calculation using these expressions and Eq. (8) is shown for  $k\ell = 13$ .

The BRAC'T computer program, whose results are most rigorous, agrees with the data within 1 dB and  $\pm 1$  deg. The analytical forms take about one minute of computer time to yield results for a given wire for all angles of incidence, while the SDI technique, competitive with the time used by the programmed analytical forms, takes a little longer, depending on the length of wire. Moreover, the general usefulness of BRAC'T becomes evident should one bend or distort the wire under consideration. Then, as expected,

the analytical expressions for the RCS do not apply to the new configuration, whereas the BRACT computer program is flexible enough so that for the most complicated configuration of a distorted thin, metallic wire, accurate results for the RCS may be obtained within a few minutes.

## REFERENCES

1. J. H. Van Vleck, F. Bloch, and M. Hamermesh, "Theory of Radar Reflections from Wires or Thin Metallic Strips," J. Appl. Phys. 18, 274 (March 1947).
2. G. T. Ruck, et al., Radar Cross Section Handbook, Vol. 1, Plenum Press, New York - London (1970).
3. C. T. Tai, "Electromagnetic Back-Scattering from Cylindrical Wires," J. Appl. Phys. 23, 909 (August 1952).
4. S. Hong, Scattering Patterns and Statistics of a Long Wire, Lincoln Lab Technical Note 1967-55 (December 1967).
5. P. Y. Ufimtsev, "Diffraction of Plane Electromagnetic Waves by a Thin Cylindrical Conductor," Radite Khnika i Electronika 7, 260 (1962), English translation, p. 241.
6. M. Rockowitz, Static Patterns of Dipoles, Lincoln Lab Project Report PA-179 (March 1971).
7. RCS Computer Program BRACT Log - Periodic Scattering Array Program, M. B. Associates, San Remon, Cal., Project No. 00041 (January 1969).
8. M. T. Tavis, Van Vleck Revisited: The RCS of Thin Wires, Aerospace Corp. Report No. TR-0073(3450-12)-1 (September 1972).

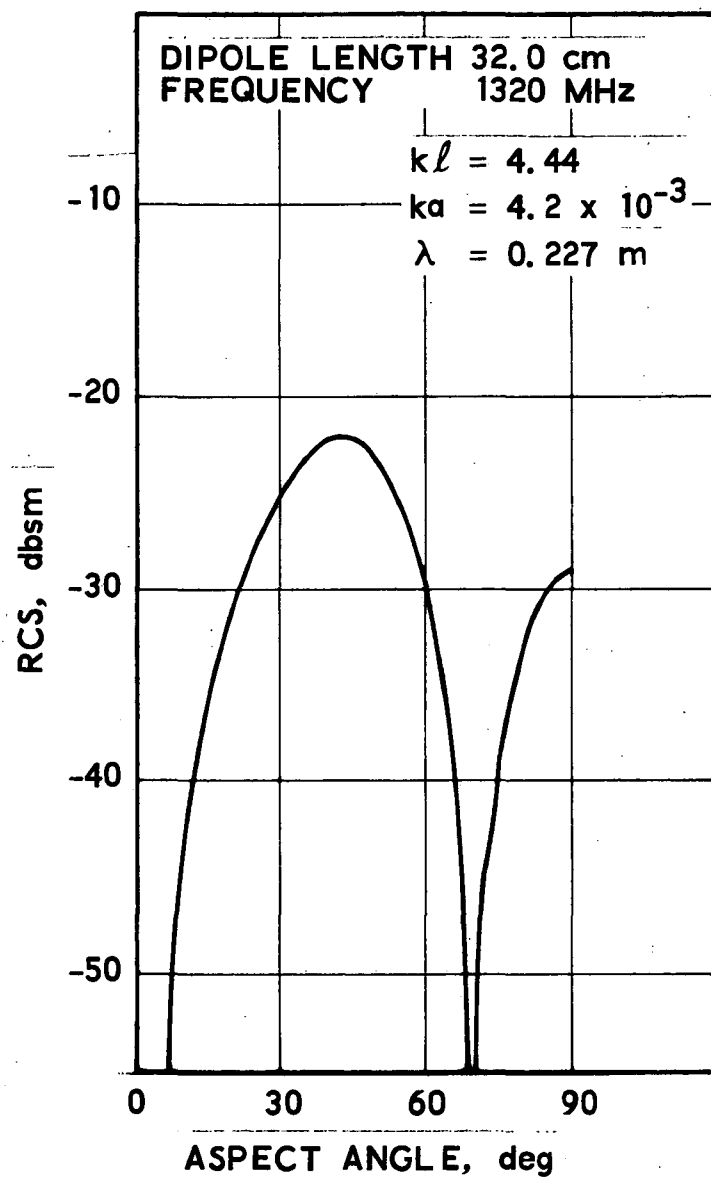


Figure 1. Measured Backscattered RCS for Thin, Metallic Straight Wires,  $k\ell = 4.44$ , Circular Polarization (90 deg corresponds to broadside)

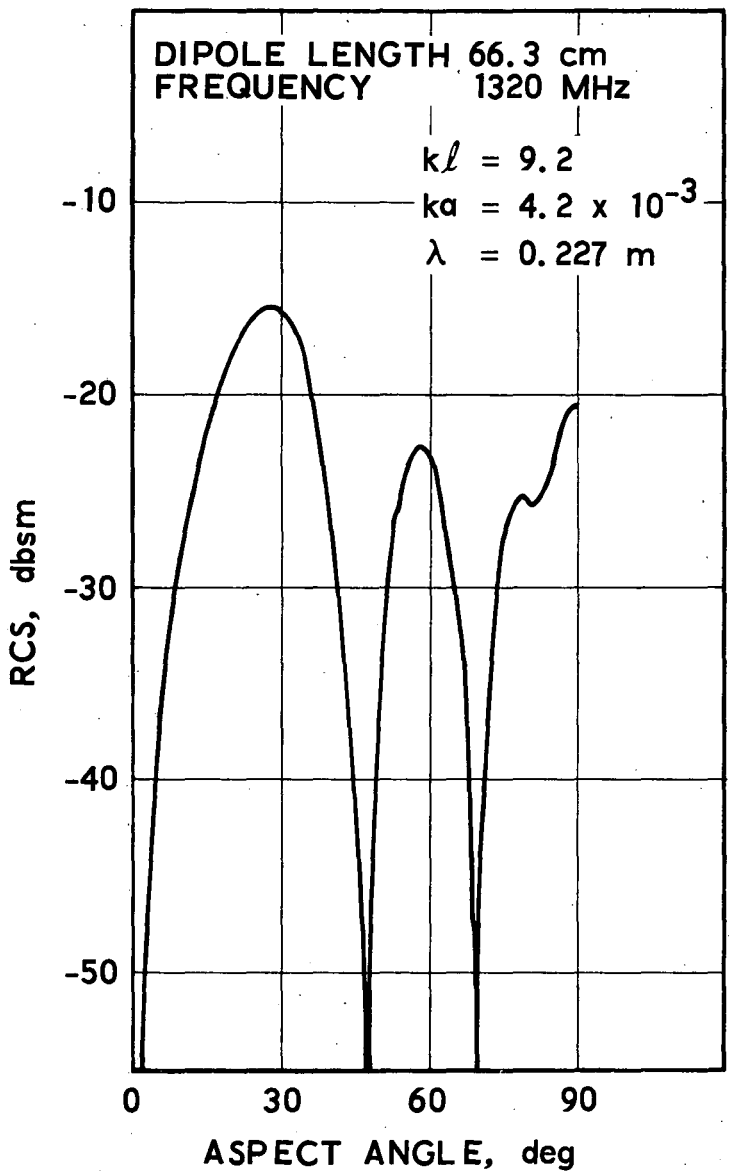


Figure 2. Measured Backscattered RCS for Thin, Metallic Straight Wires,  $k\ell = 9.2$ , Circular Polarization (90 deg corresponds to broadside)

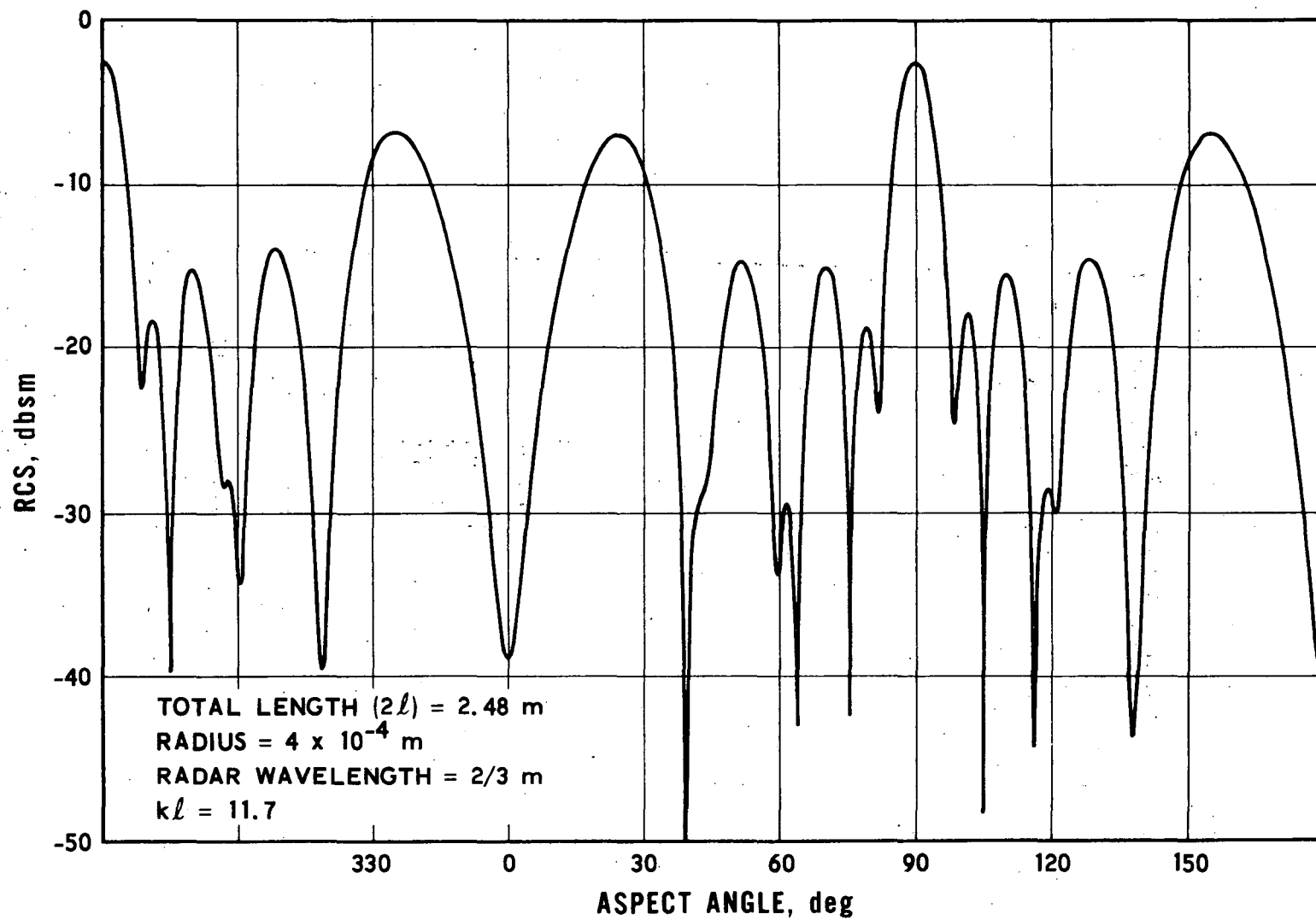


Figure 3. Measured Backscattered RCS for Thin, Metallic Straight Wires,  $k\ell = 11.7$ , Linear Polarization (90 deg corresponds to broadside)

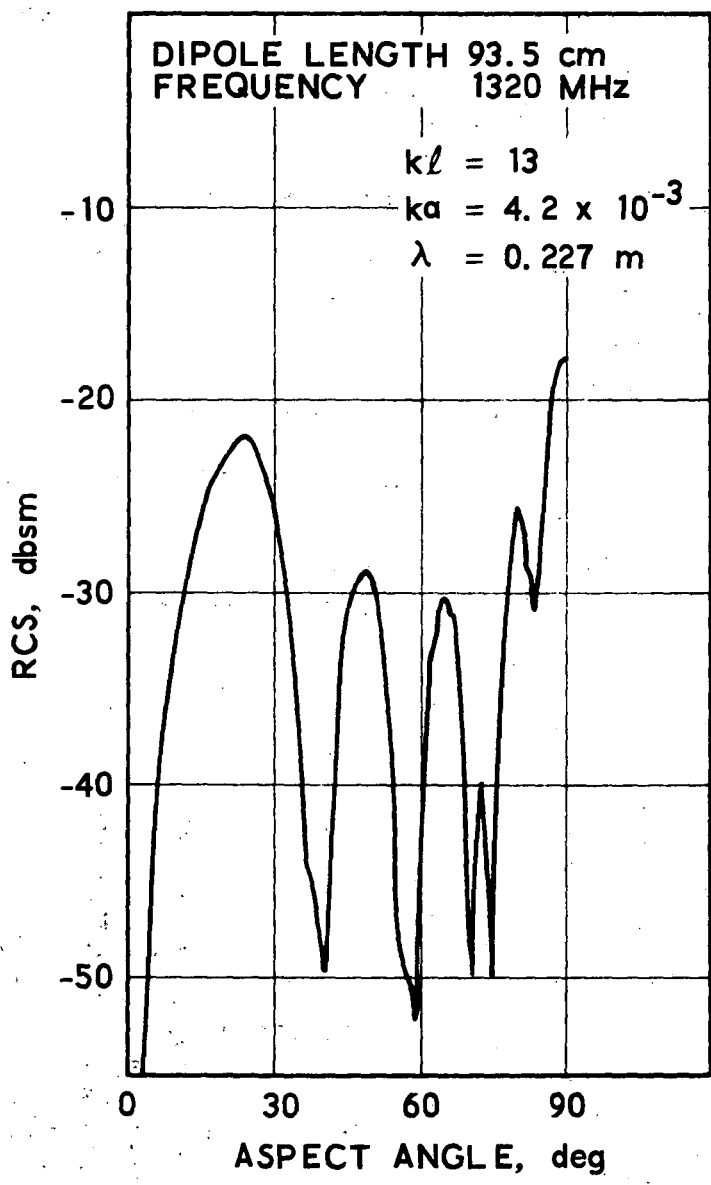


Figure 4. Measured Backscattered RCS for Thin, Metallic Straight Wires,  $k\ell = 13$ , Circular Polarization (90 deg corresponds to broadside)

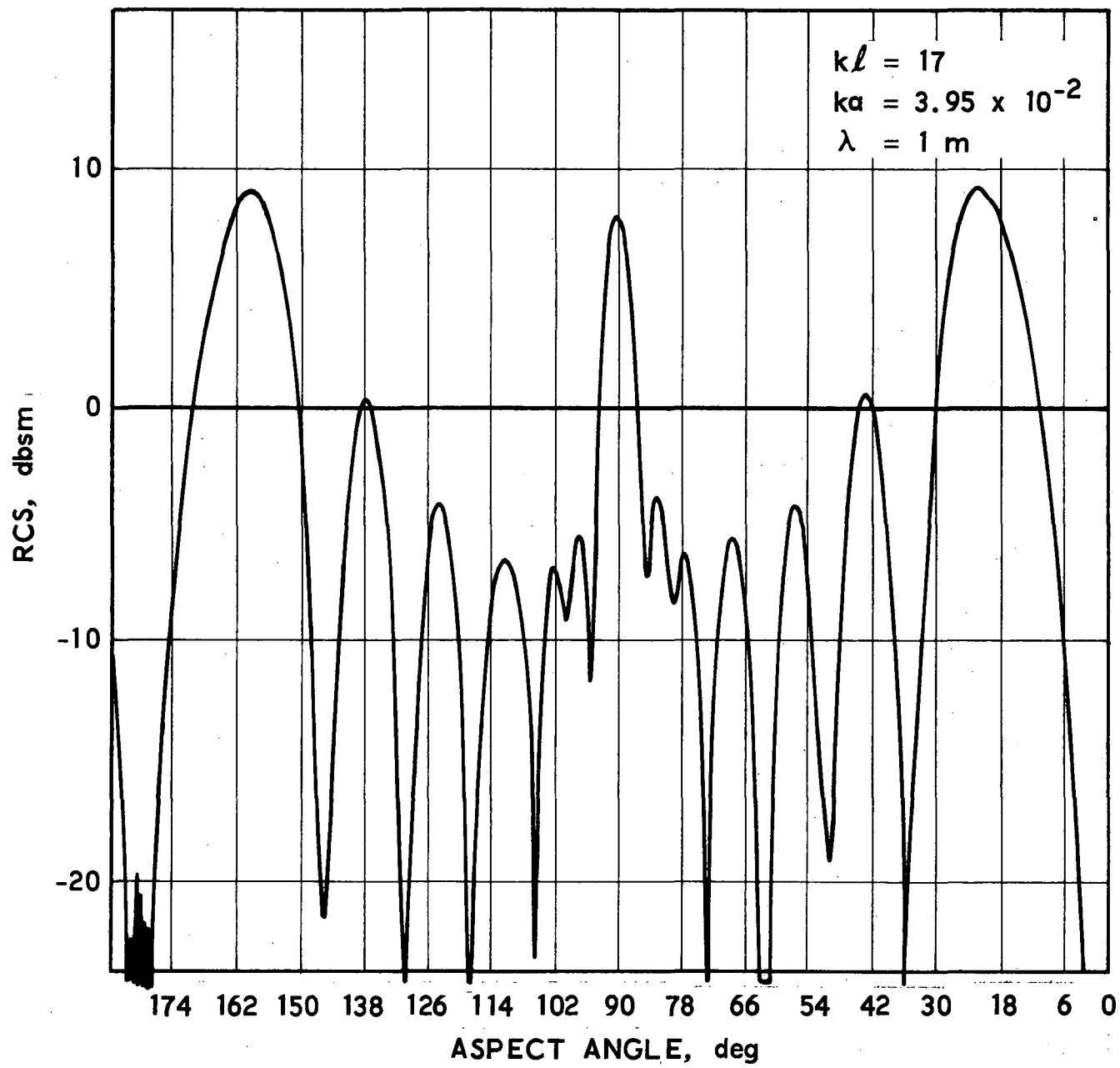


Figure 5. Measured Backscattered RCS for Thin, Metallic Straight Wires,  $k\ell = 17$ , Linear Polarization (90 deg corresponds to broadside)

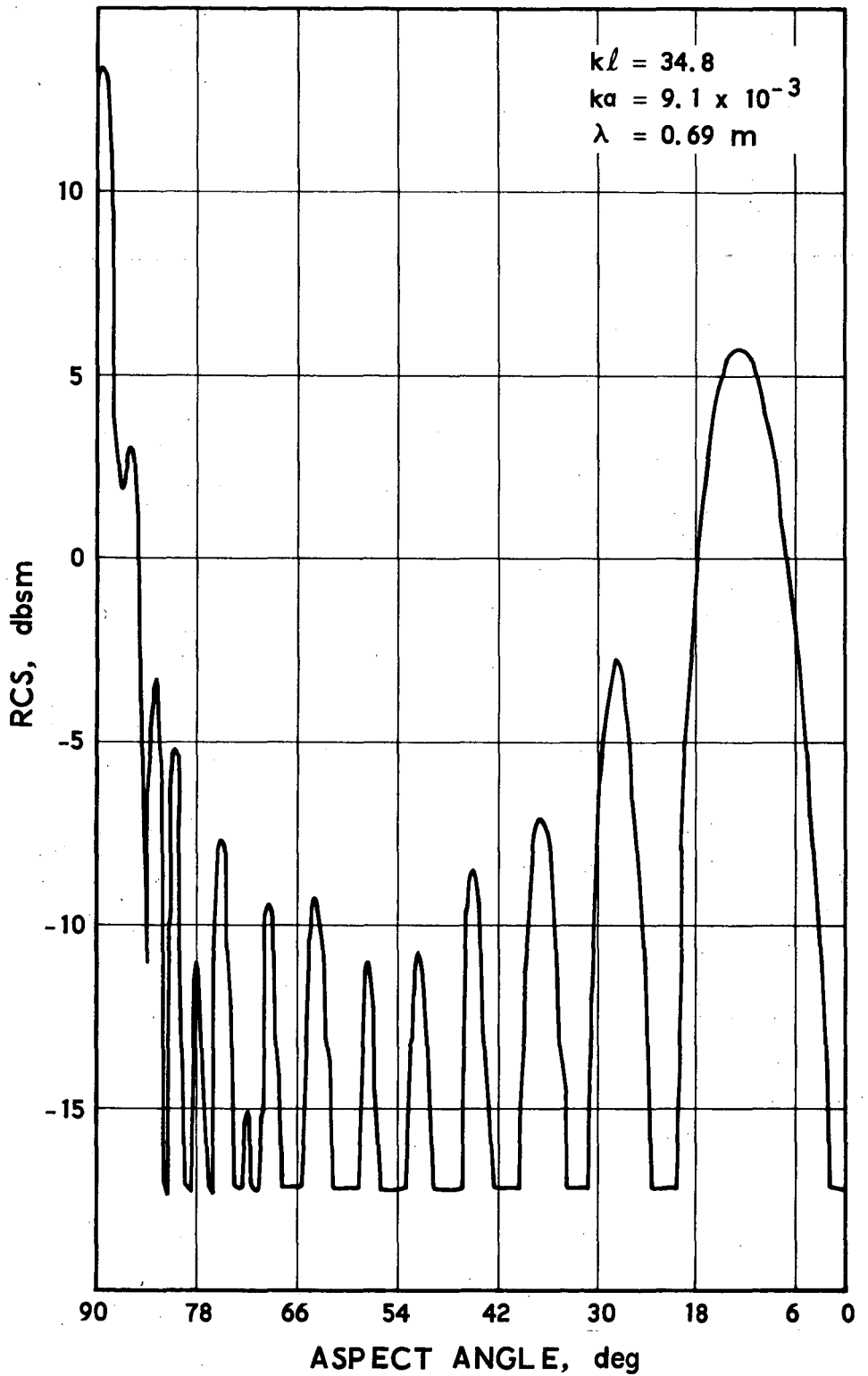


Figure 6. Measured Backscattered RCS for Thin, Metallic Straight Wires,  $k\ell = 34.8$ , Linear Polarization (90 deg corresponds to broadside)

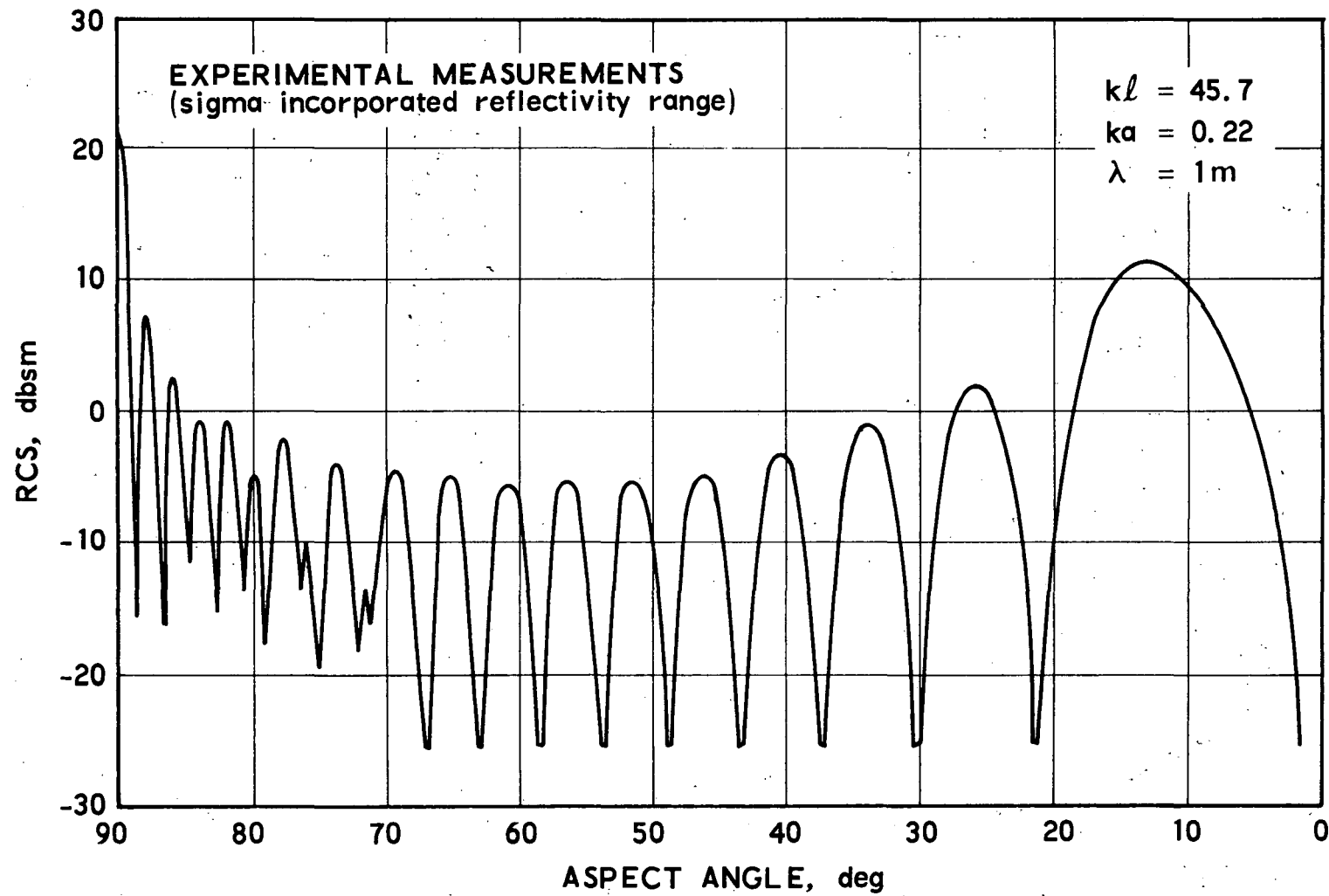


Figure 7. Measured Backscattered RCS for Thin, Metallic Straight Wires,  $k\ell = 45.7$ , Linear Polarization (90 deg corresponds to broadside)

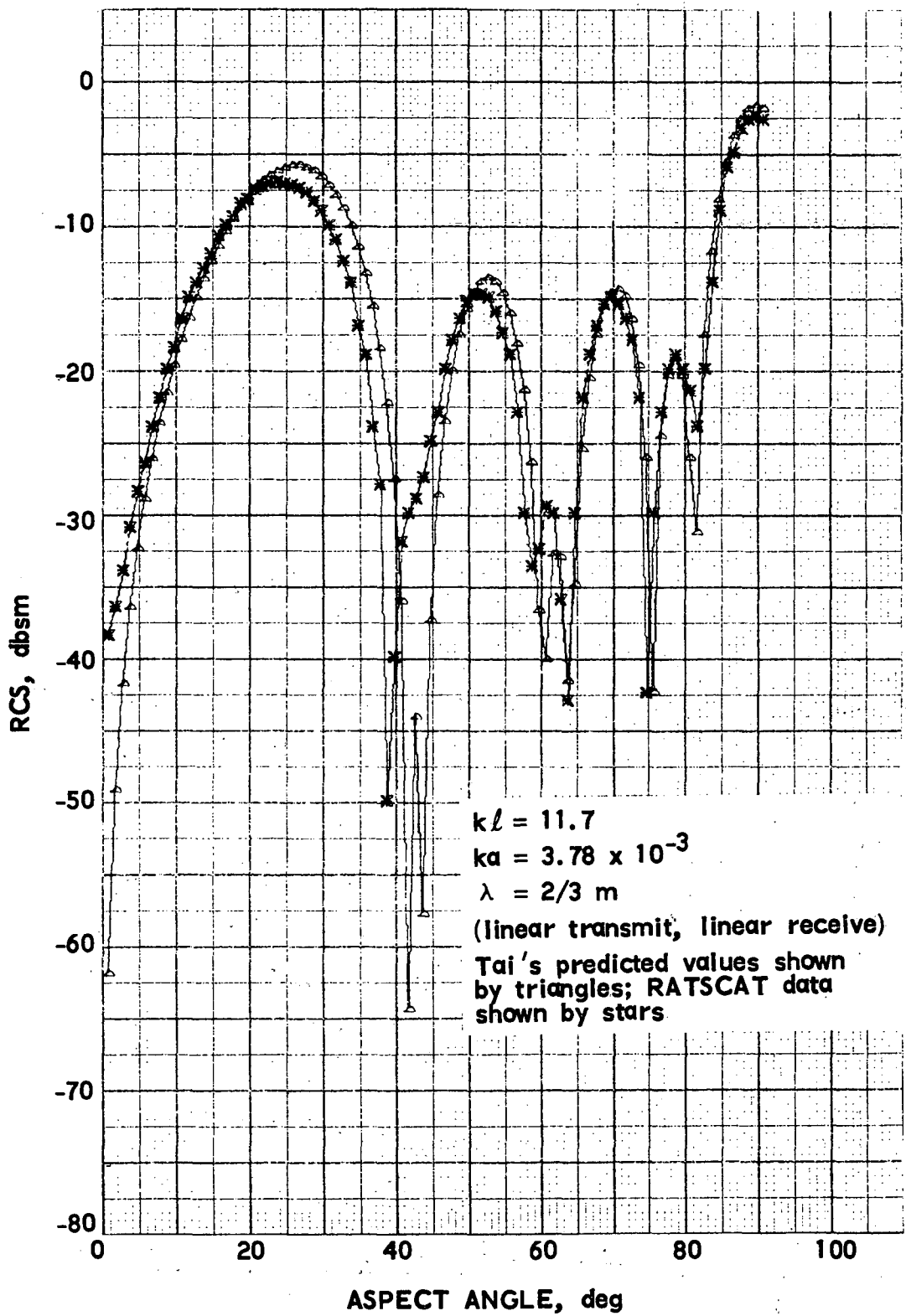


Figure 8. Comparison of Tai's Predicted RCS with Measured Data,  $k\ell = 11.7$

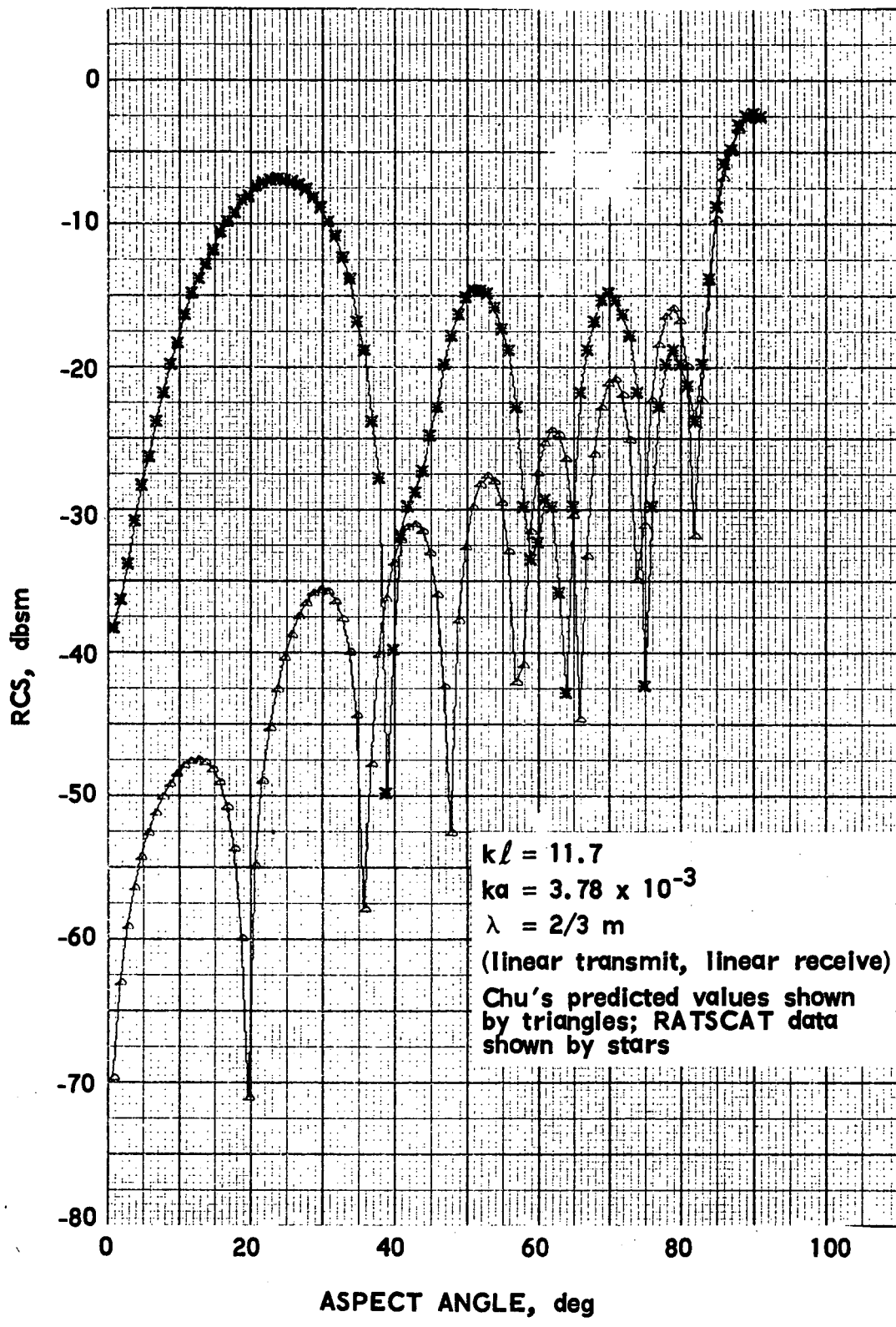


Figure 9. Comparison of Chu's Predicted RCS with Measured Data,  $k\ell = 11.7$

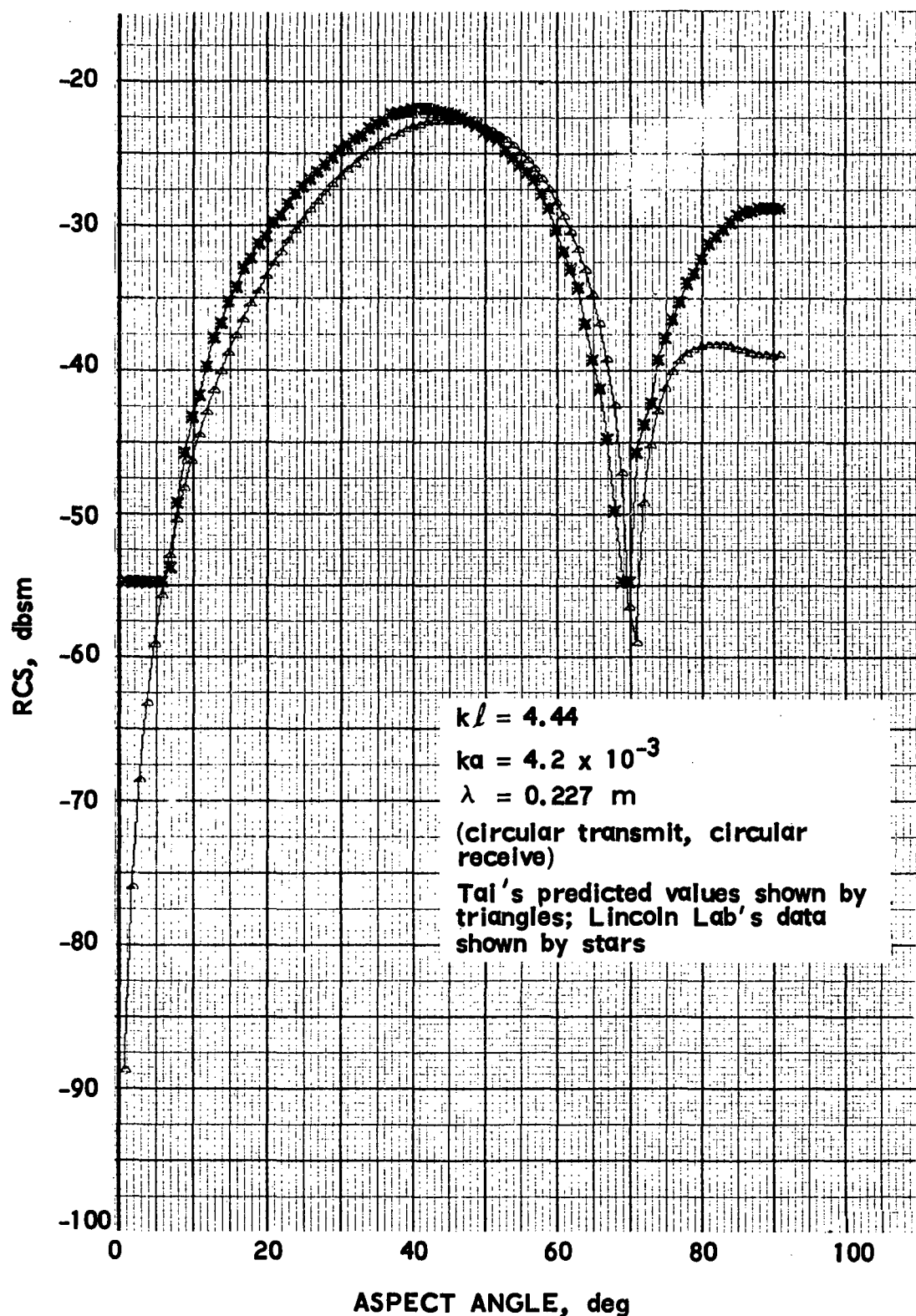


Figure 10. Comparison of Tai's Prediction with Measured RCS Data,  $k\ell = 4.44$

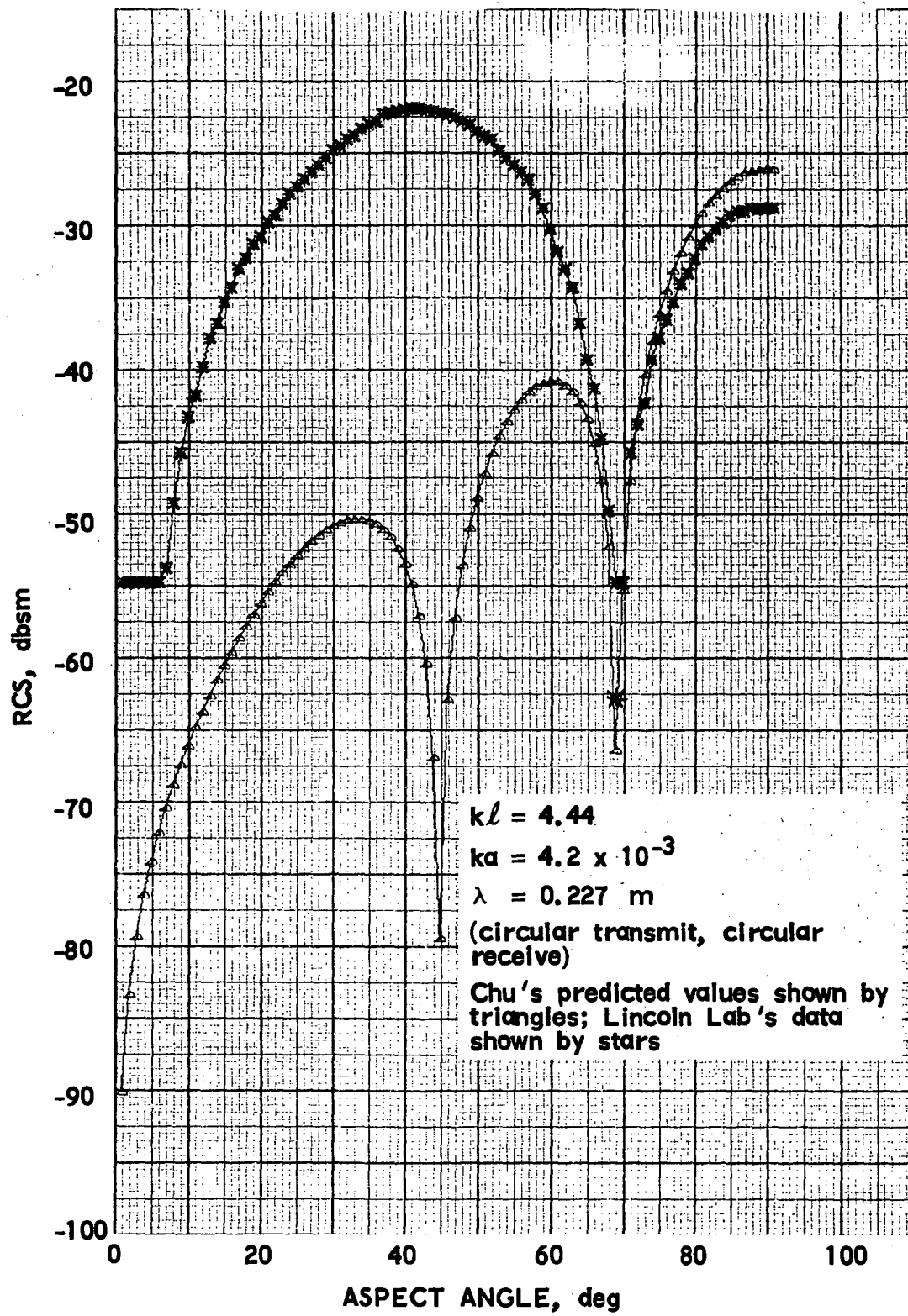


Figure 11. Comparison of Chu's Predicted RCS with Measured Data,  $kl = 4.44$

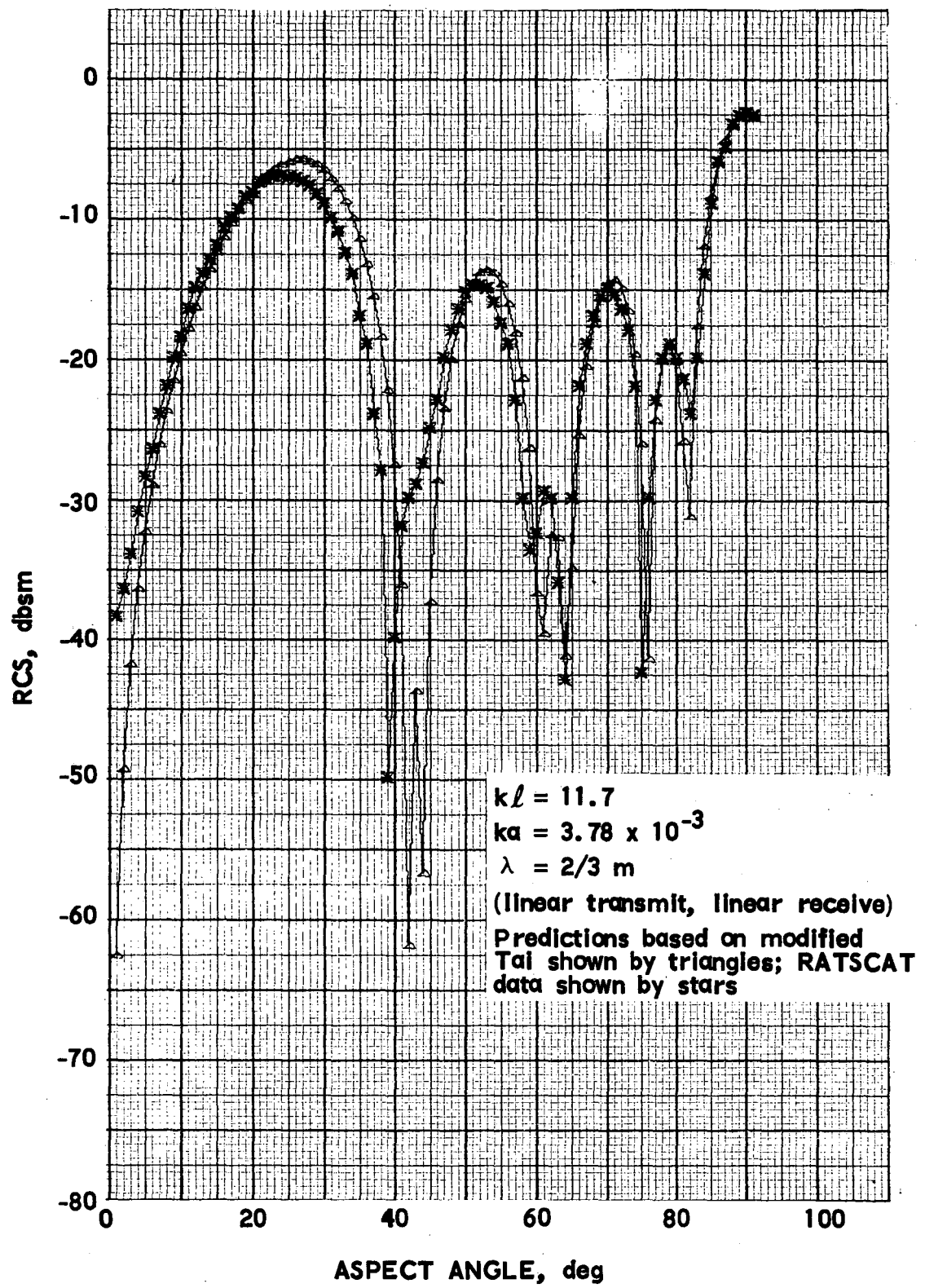


Figure 12. Comparison of Modified Tai's Prediction with Measured RCS Data,  $k\ell = 11.7$

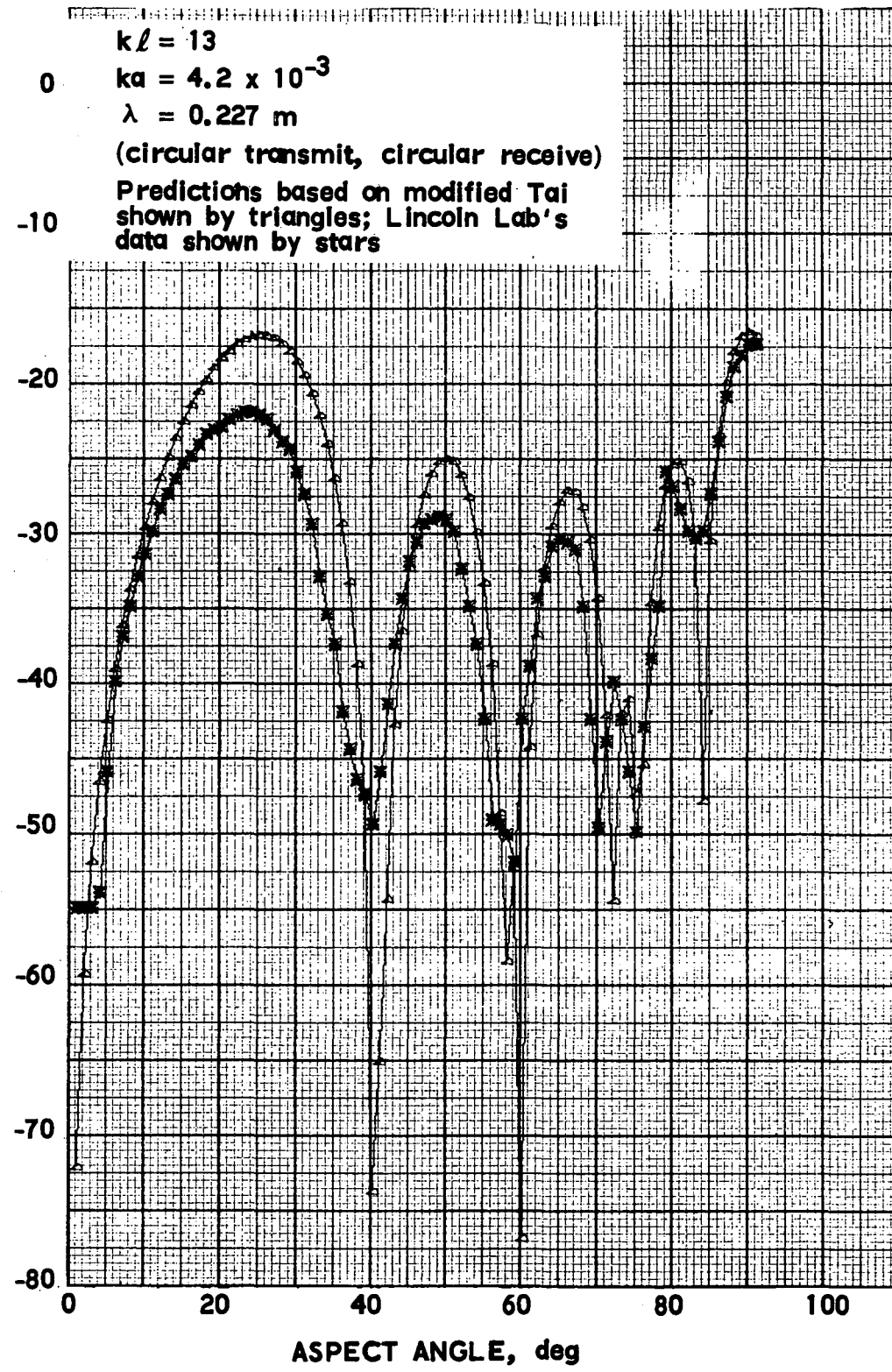


Figure 13. Comparison of Modified Tai's Prediction with Measured RCS Data,  $k\ell = 13$

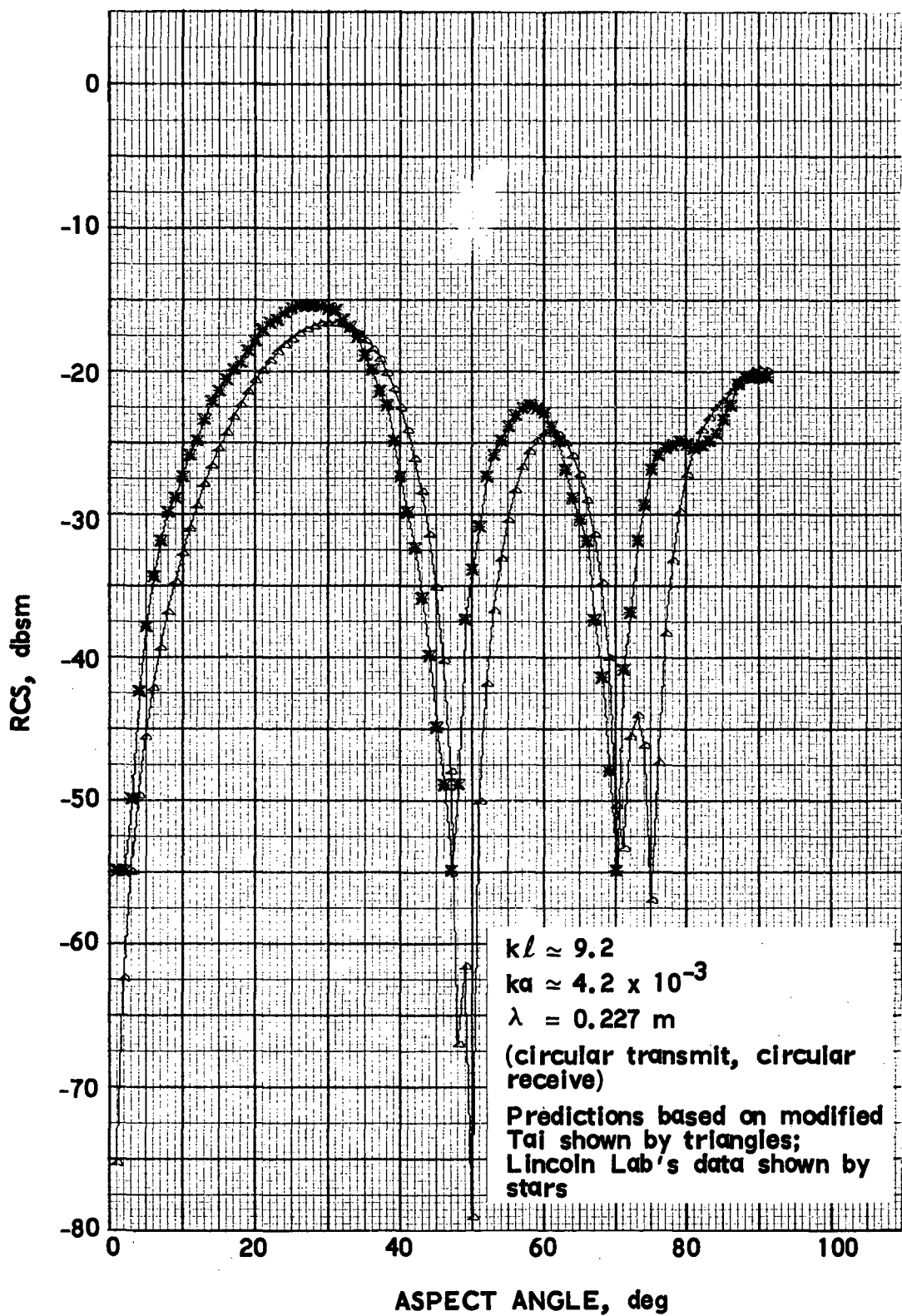


Figure 14. Comparison of Modified Tai's Prediction with Measured RCS Data,  $k\ell = 9.2$

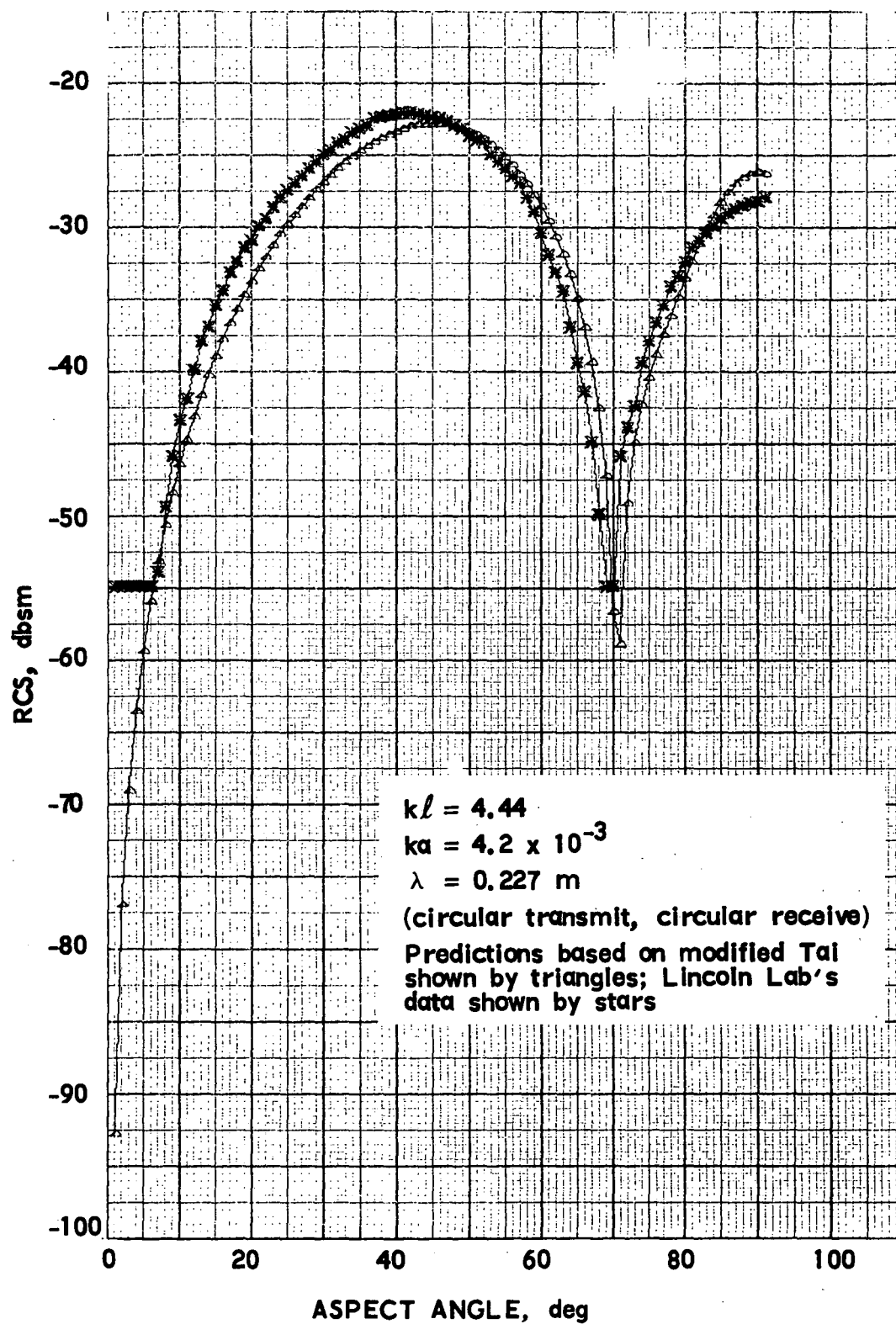


Figure 15. Comparison of Modified Tai's Predicted RCS with Measured Data,  $k\ell = 4.44$

$k\ell = 17$   
 $ka = 3.95 \times 10^{-2}$   
20 scaled to  $\lambda = 1$  m  
(transmit circular, receive circular)  
Predictions based on modified Tai  
shown by triangles; University of  
Michigan data shown by stars

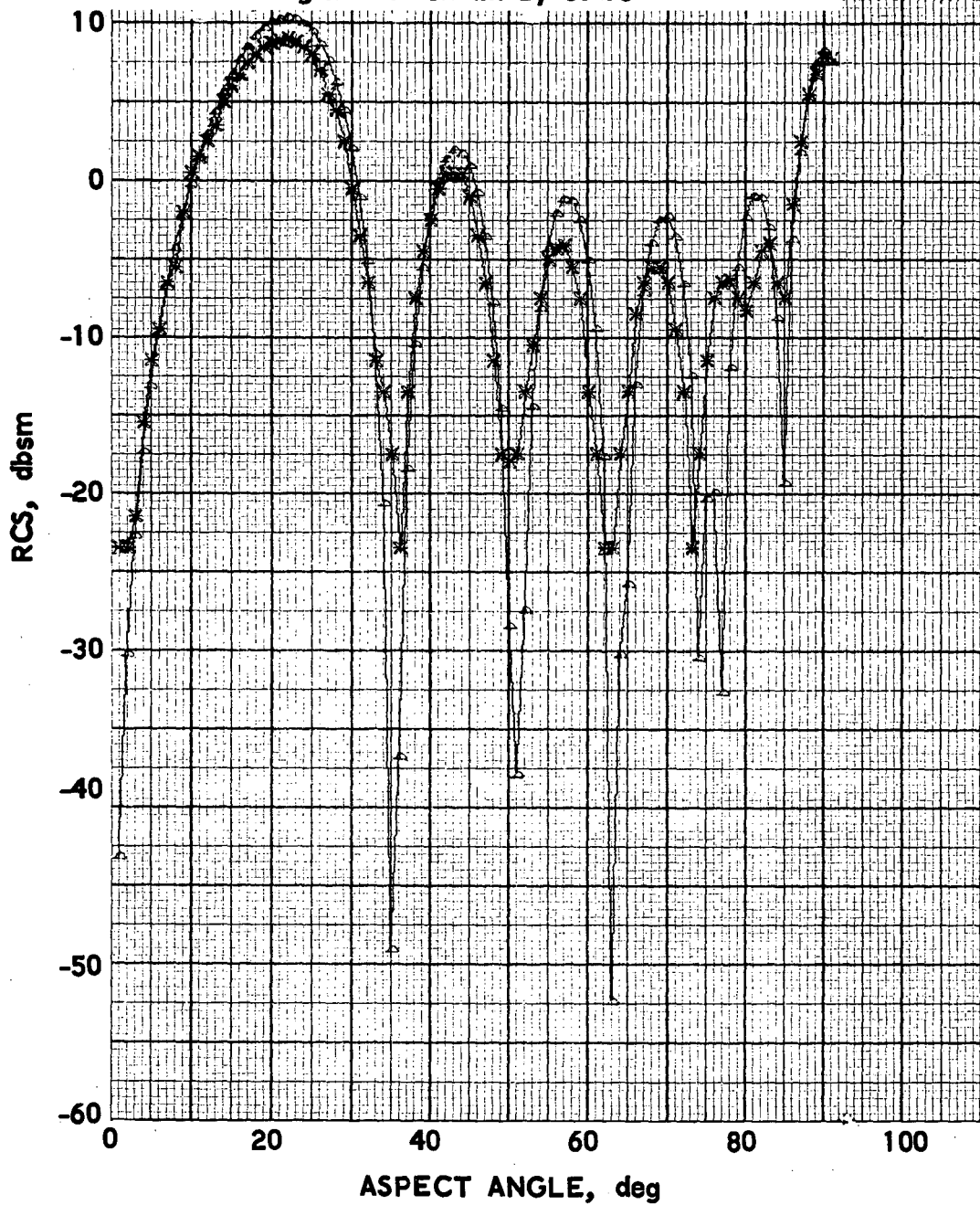


Figure 16. Comparison of Modified Tai's Prediction with Measured RCS Data,  $k\ell = 17$

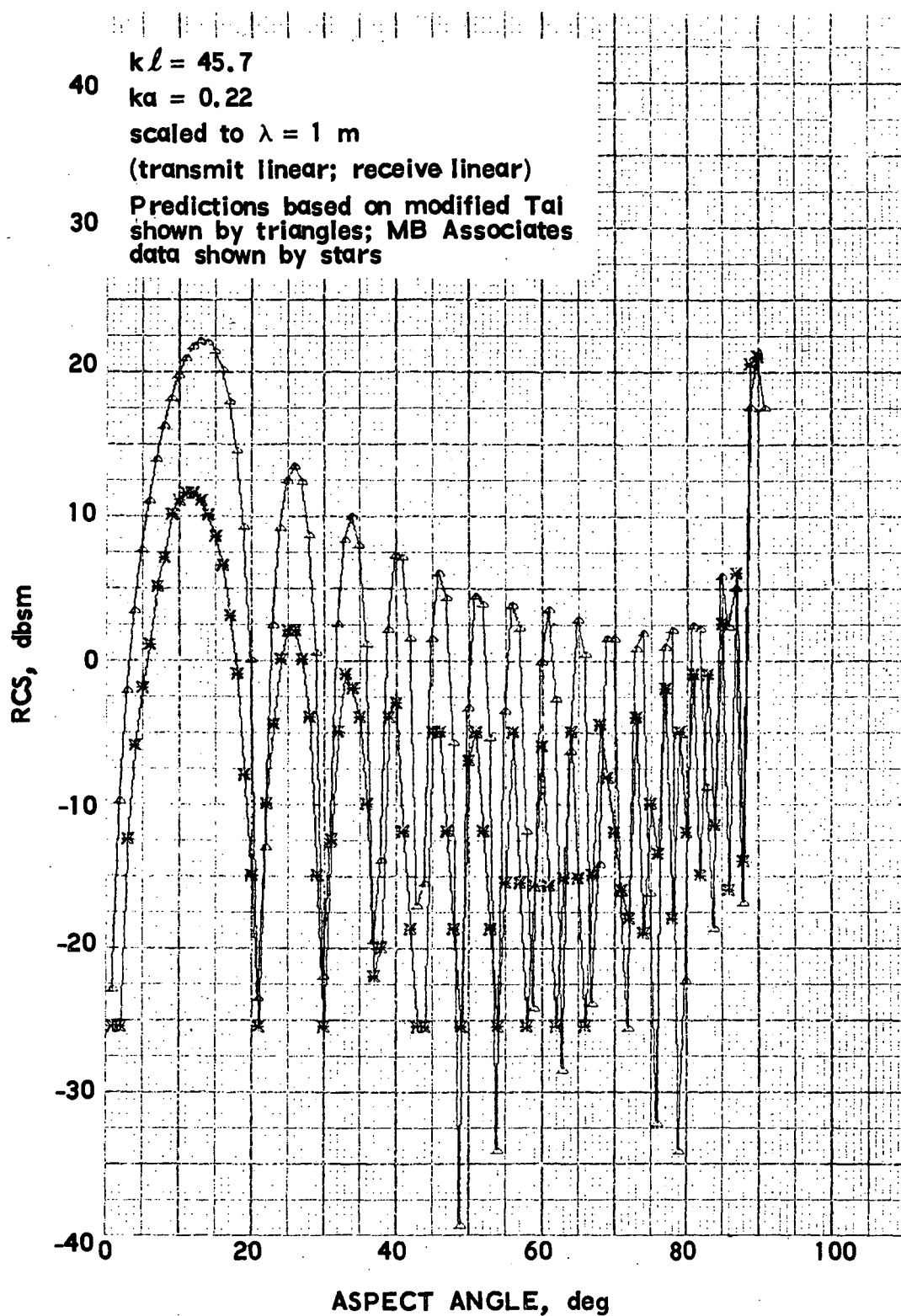


Figure 17. Comparison of Modified Tai's Prediction with Measured RCS Data,  $kl = 45.7$

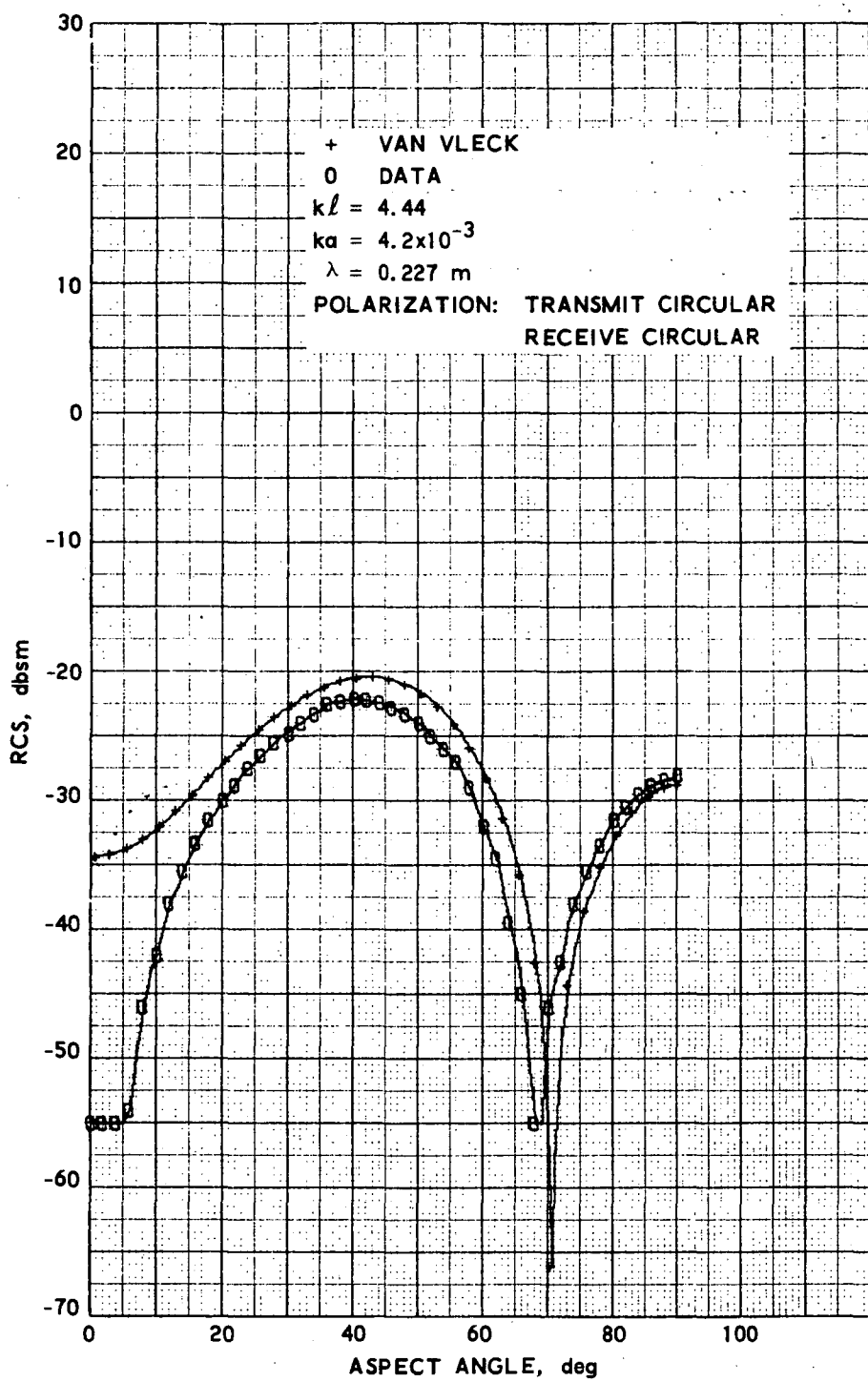


Figure 18. Comparison of Van Vleck's Predicted RCS with Measured Data,  $k'l = 4.44$

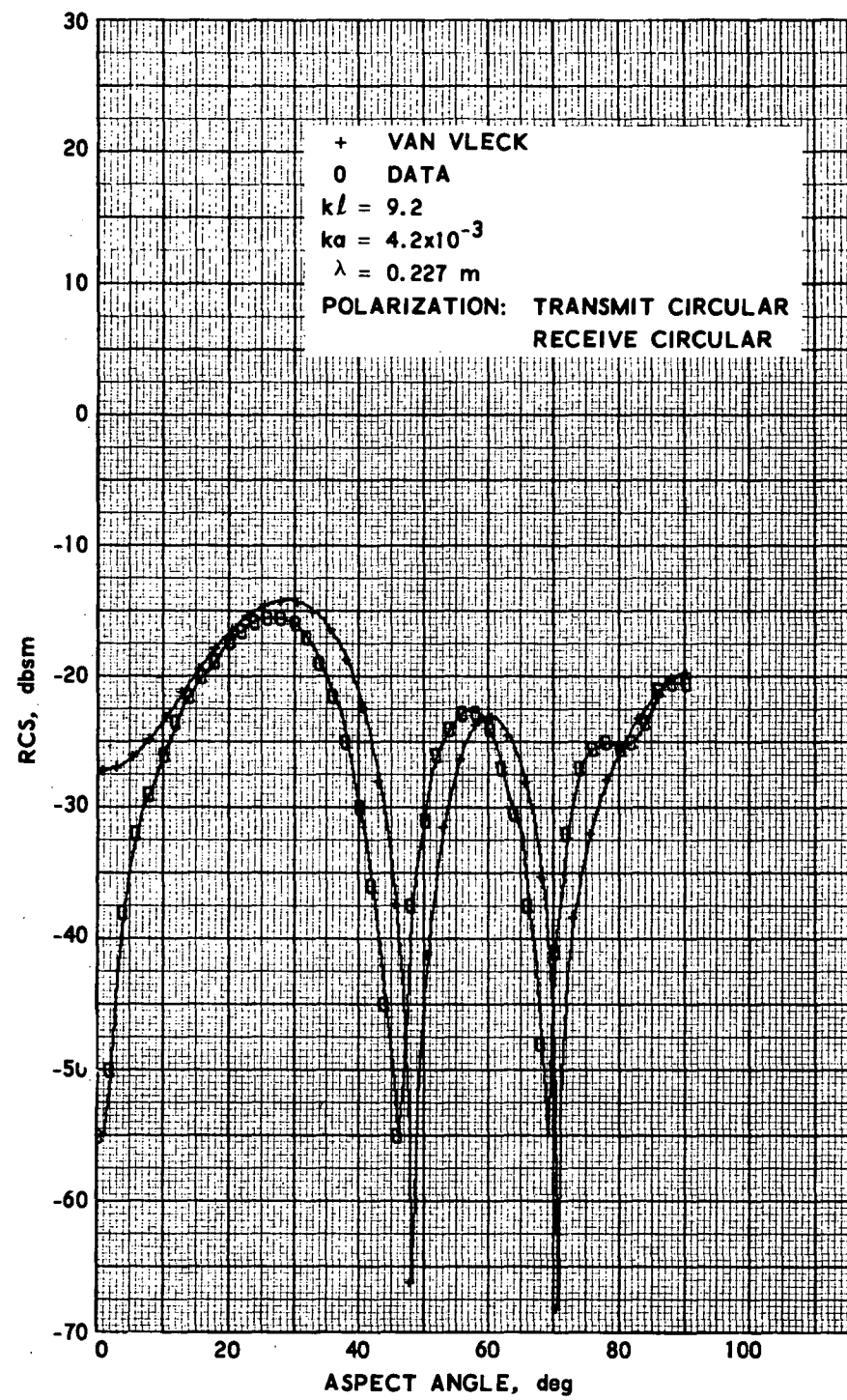


Figure 19. Comparison of Van Vleck's Predicted RCS with Measured Data,  $kl = 9.2$

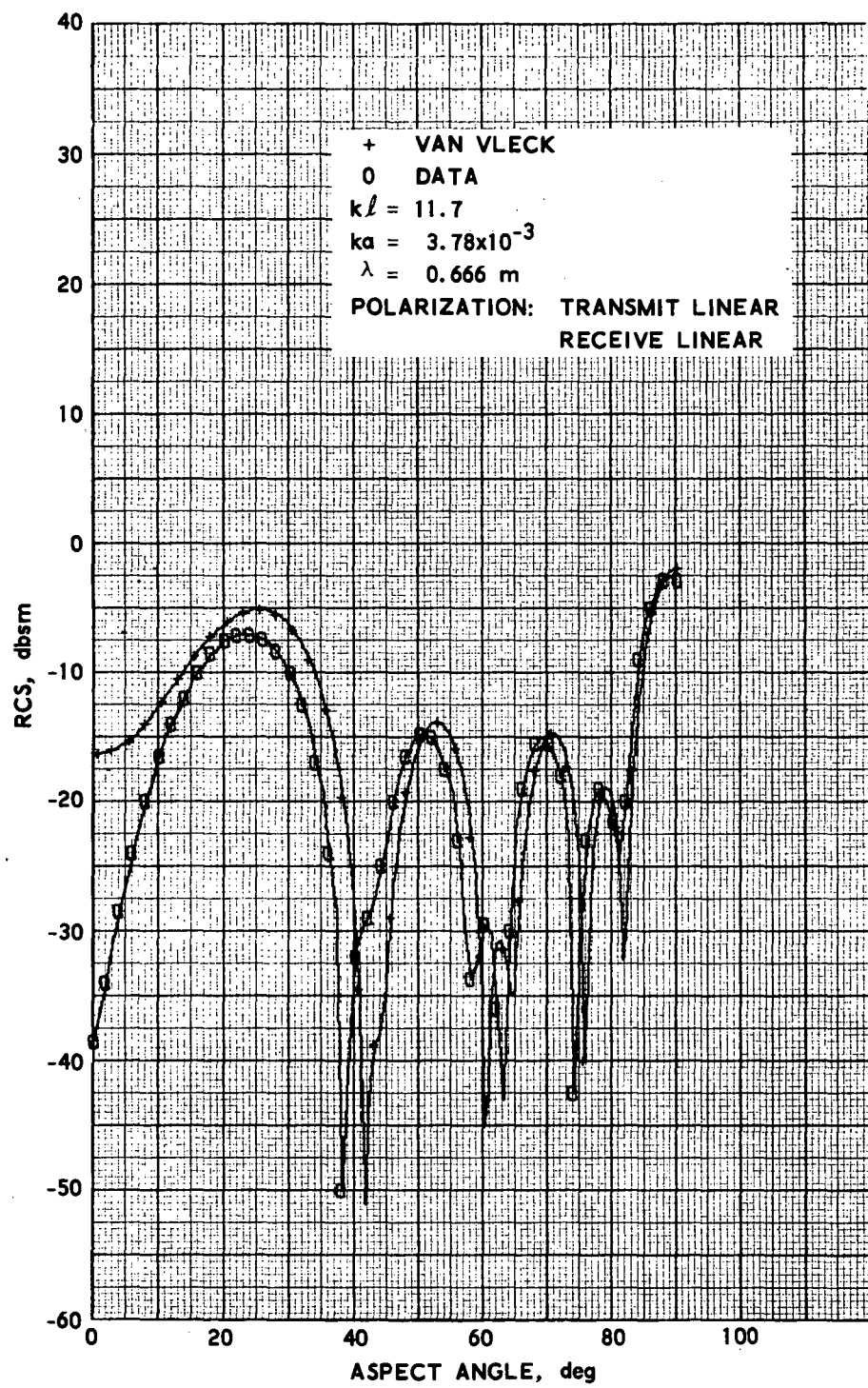


Figure 20. Comparison of Van Vleck's Predicted RCS with Measured Data,  $k'l = 11.7$

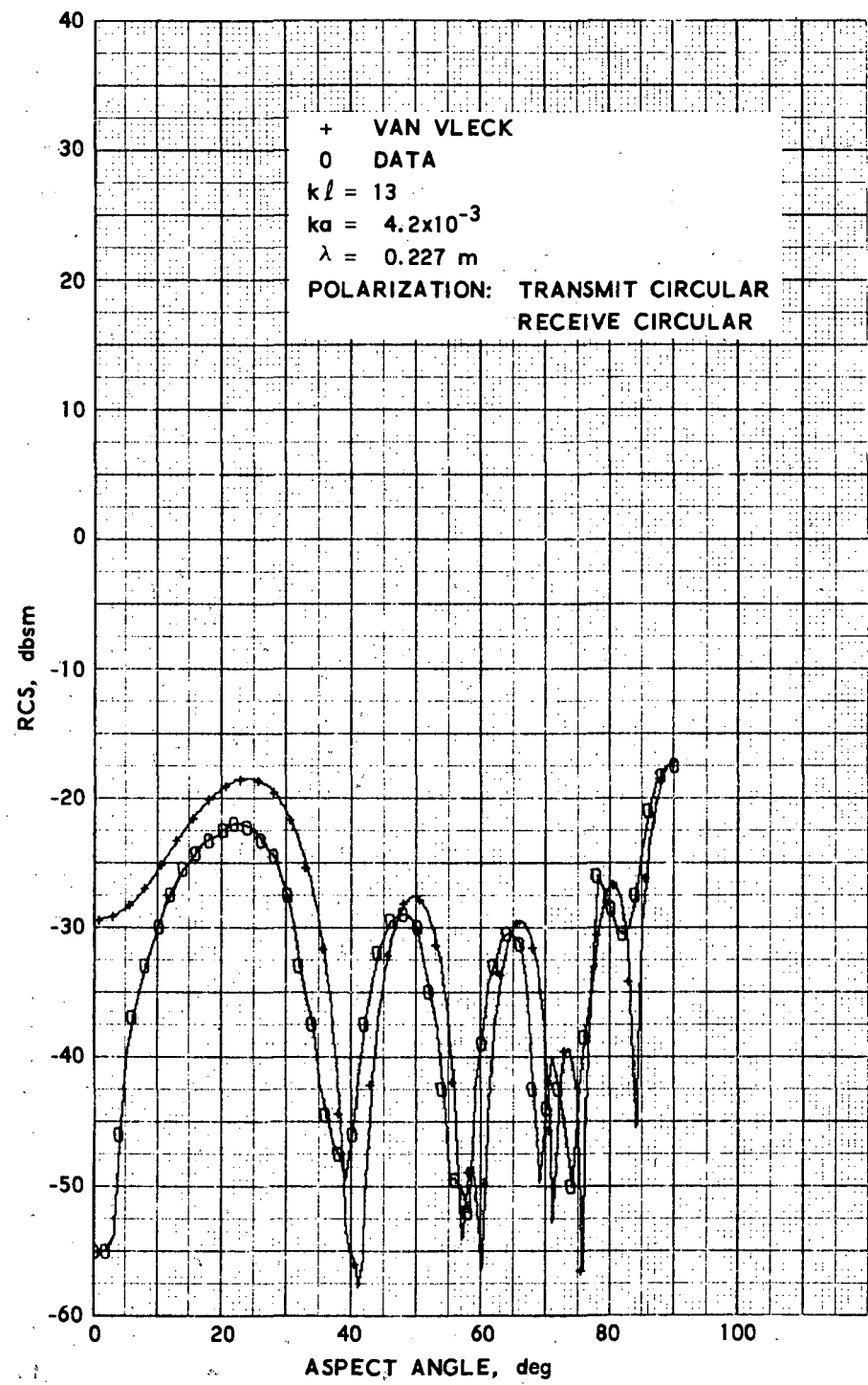


Figure 21. Comparison of Van Vleck's Predicted RCS with Measured Data,  $k\ell = 13$

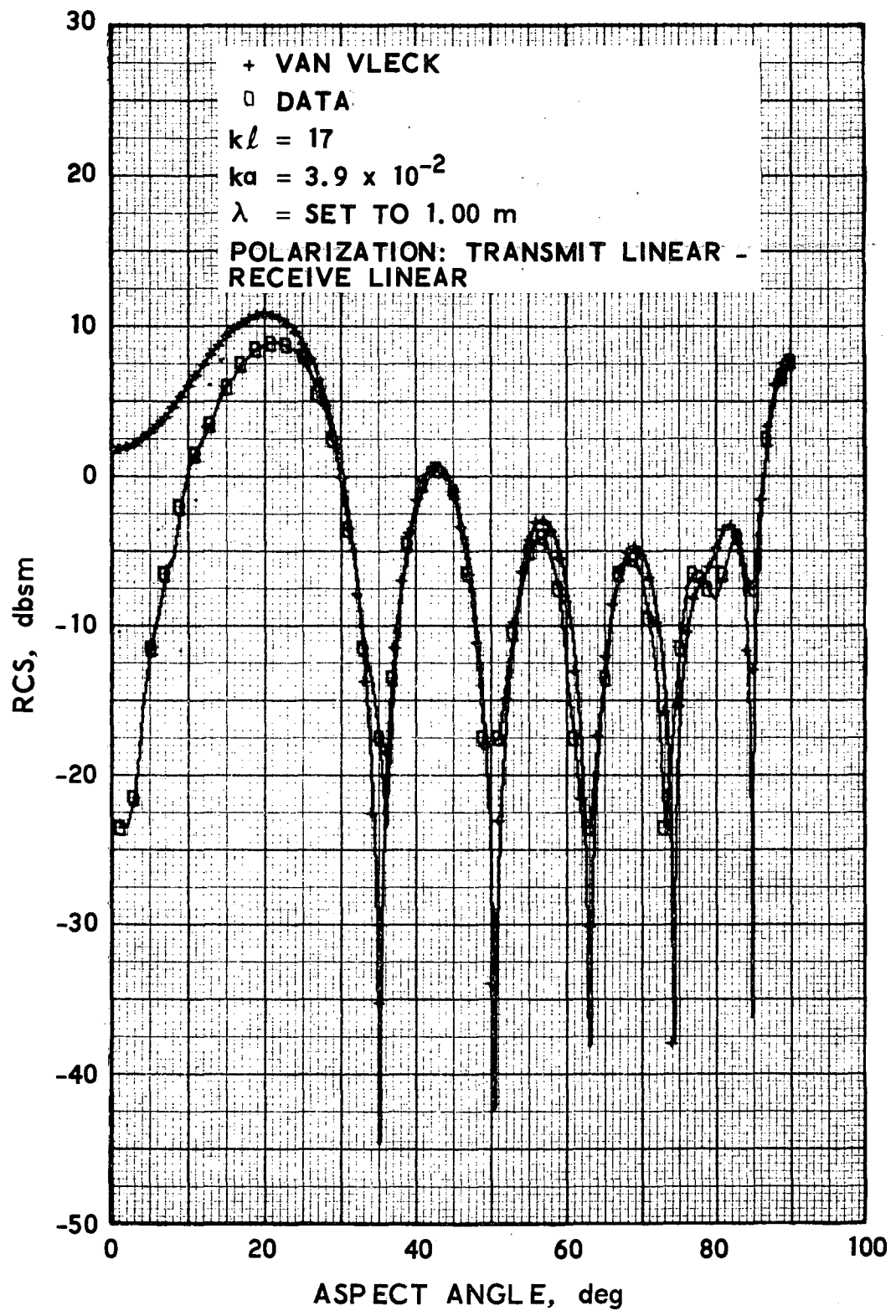


Figure 22. Comparison of Van Vleck's Predicted RCS with Measured Data,  $k\ell = 17$

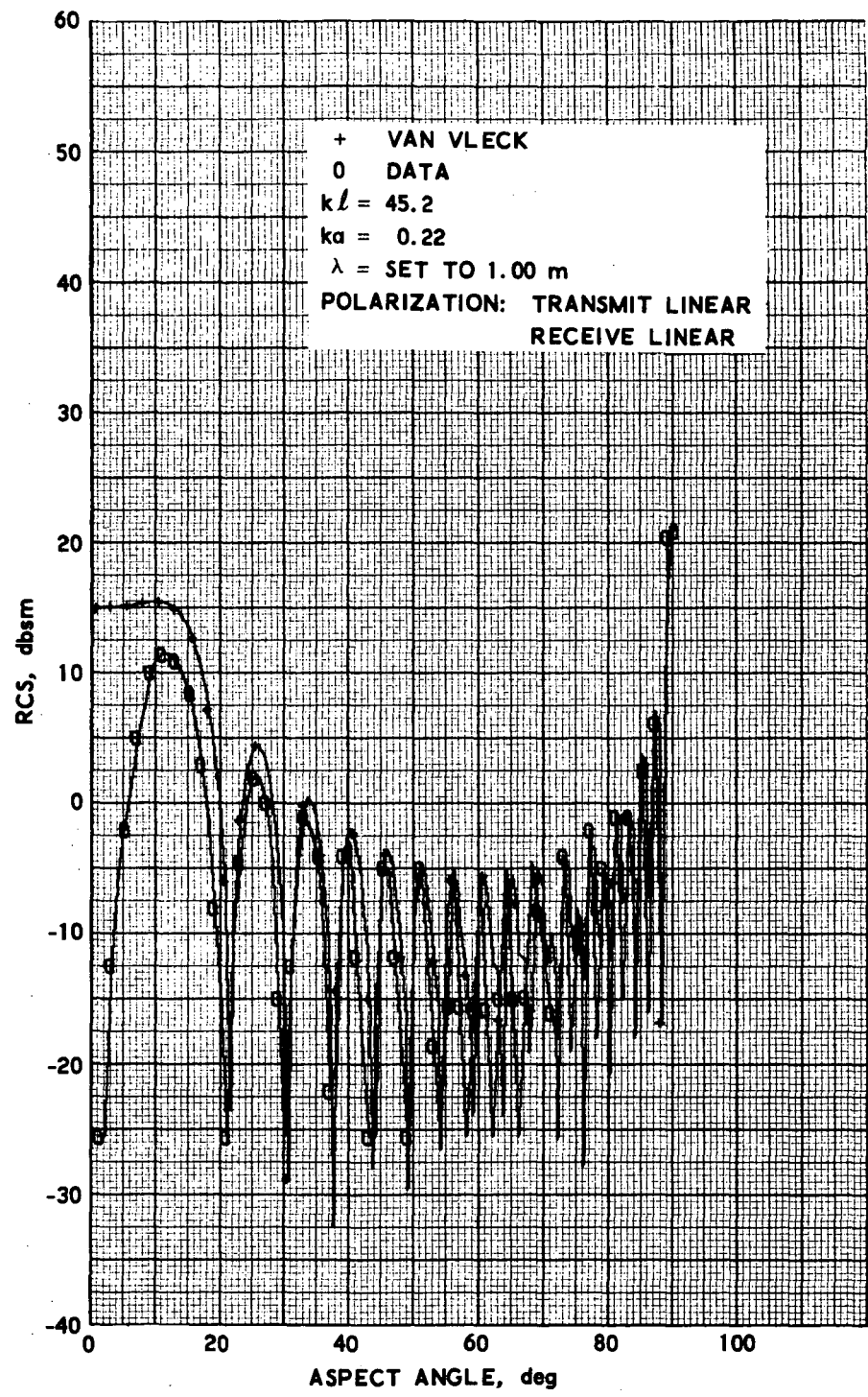


Figure 23. Comparison of Van Vleck's Predicted RCS with Measured Data,  $kl = 45.2$

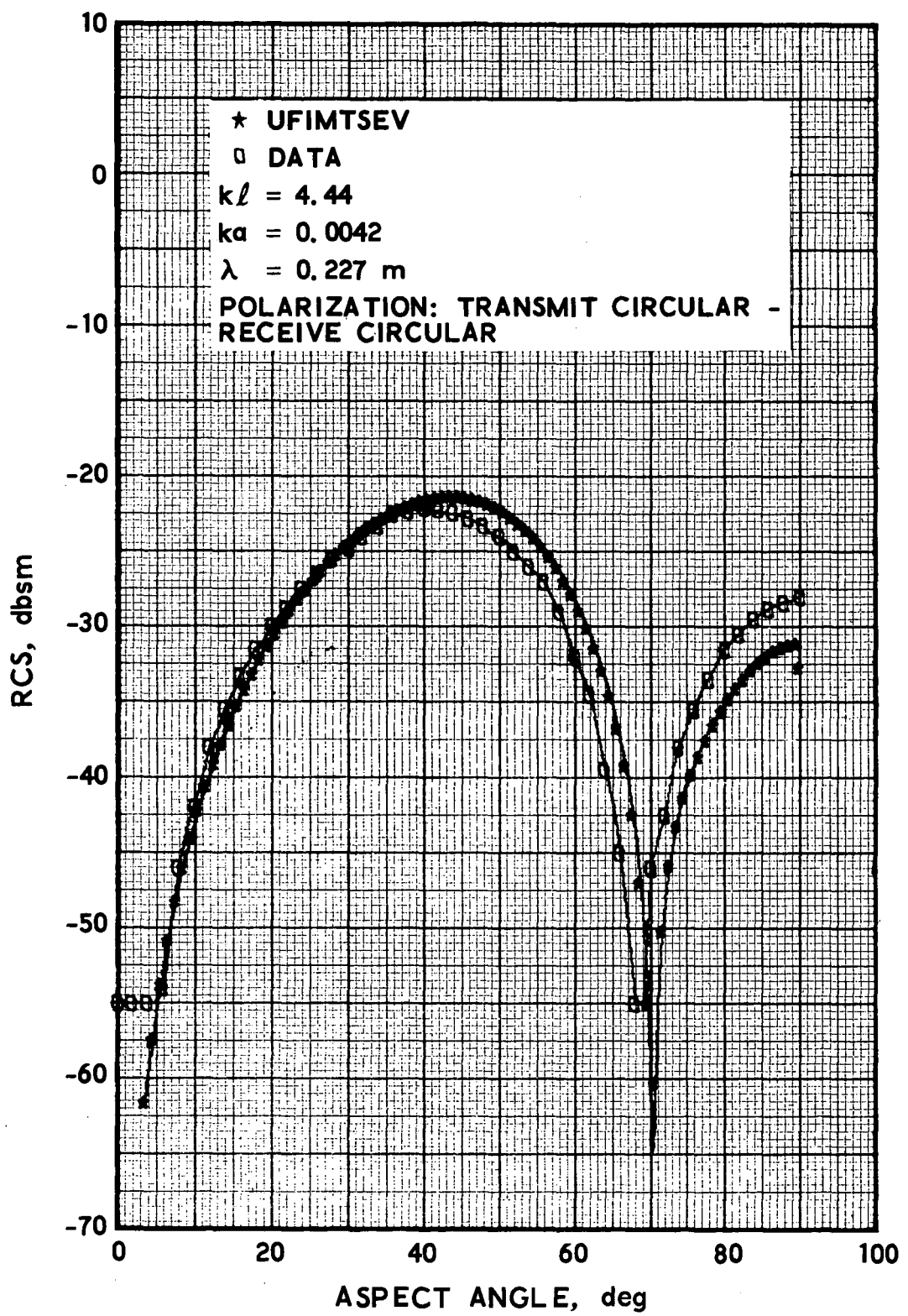


Figure 24. Comparison of Ufimtsev's Predicted RCS with Measured Data,  $kl = 4.44$

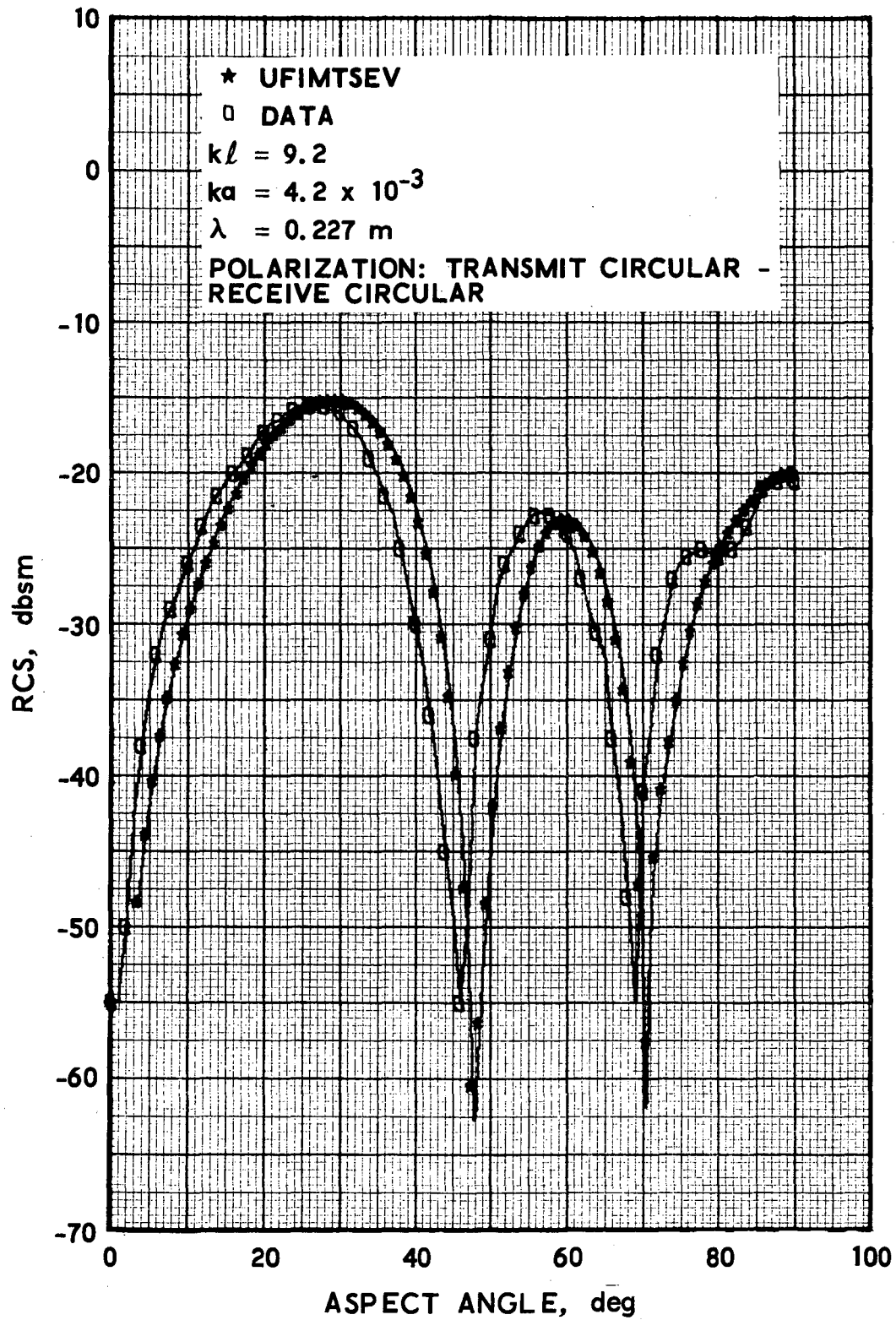


Figure 25. Comparison of Ufimtsev's Predicted RCS with Measured Data,  $k\ell = 9.2$

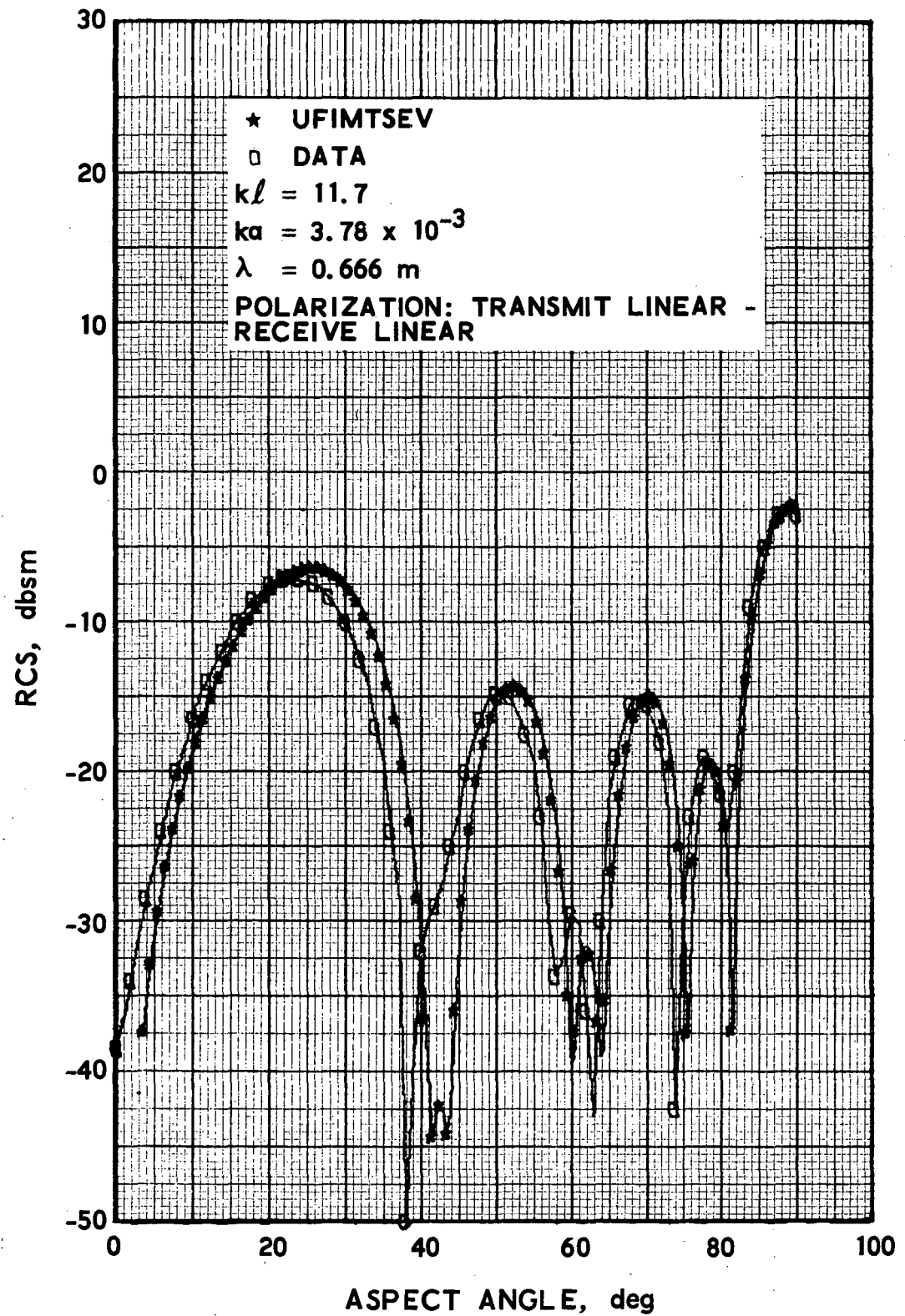


Figure 26. Comparison of Ufimtsev's Predicted RCS with Measured Data,  $k\ell = 11.7$

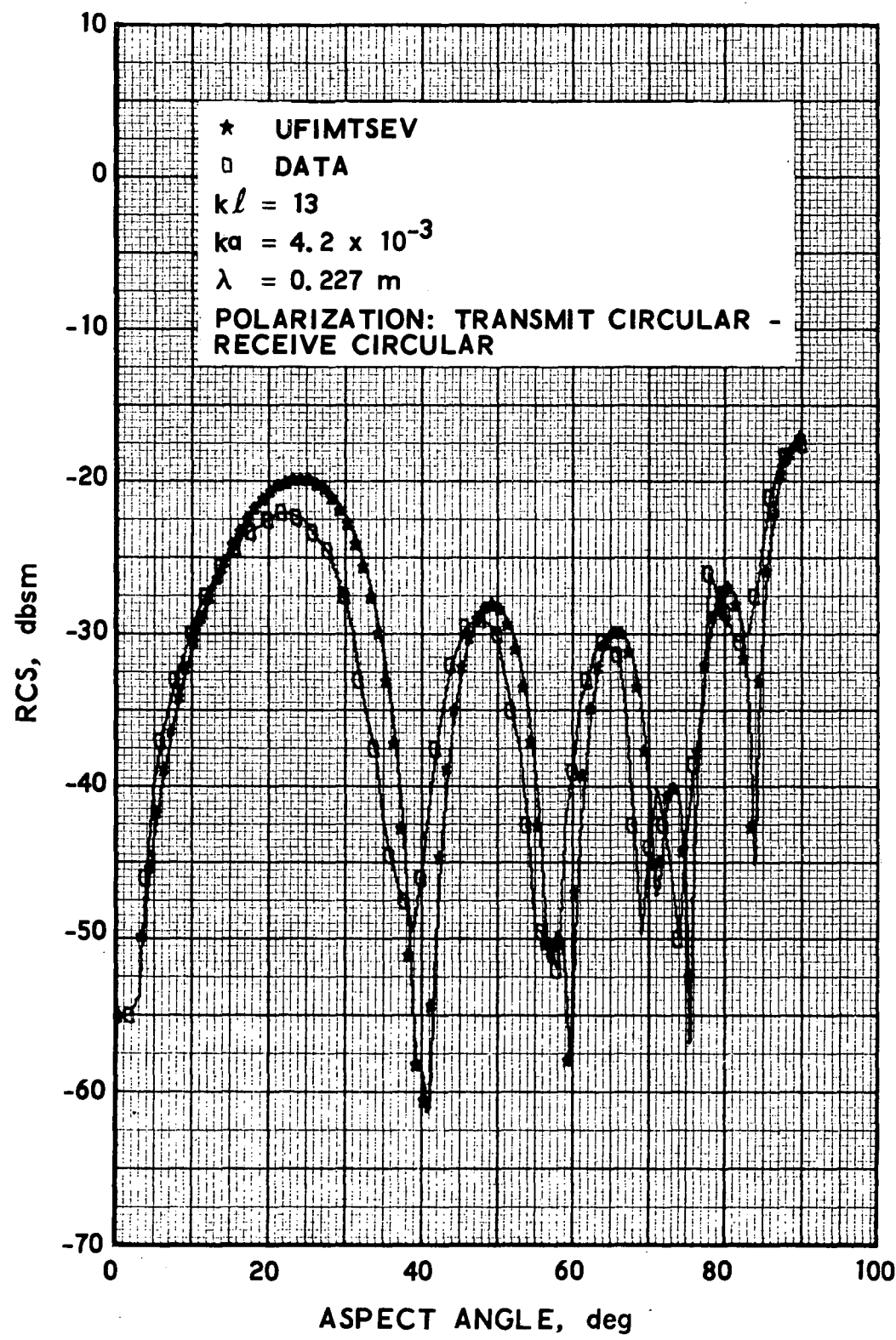


Figure 27. Comparison of Ufimtsev's Predicted RCS with Measured Data,  $k\ell = 13$

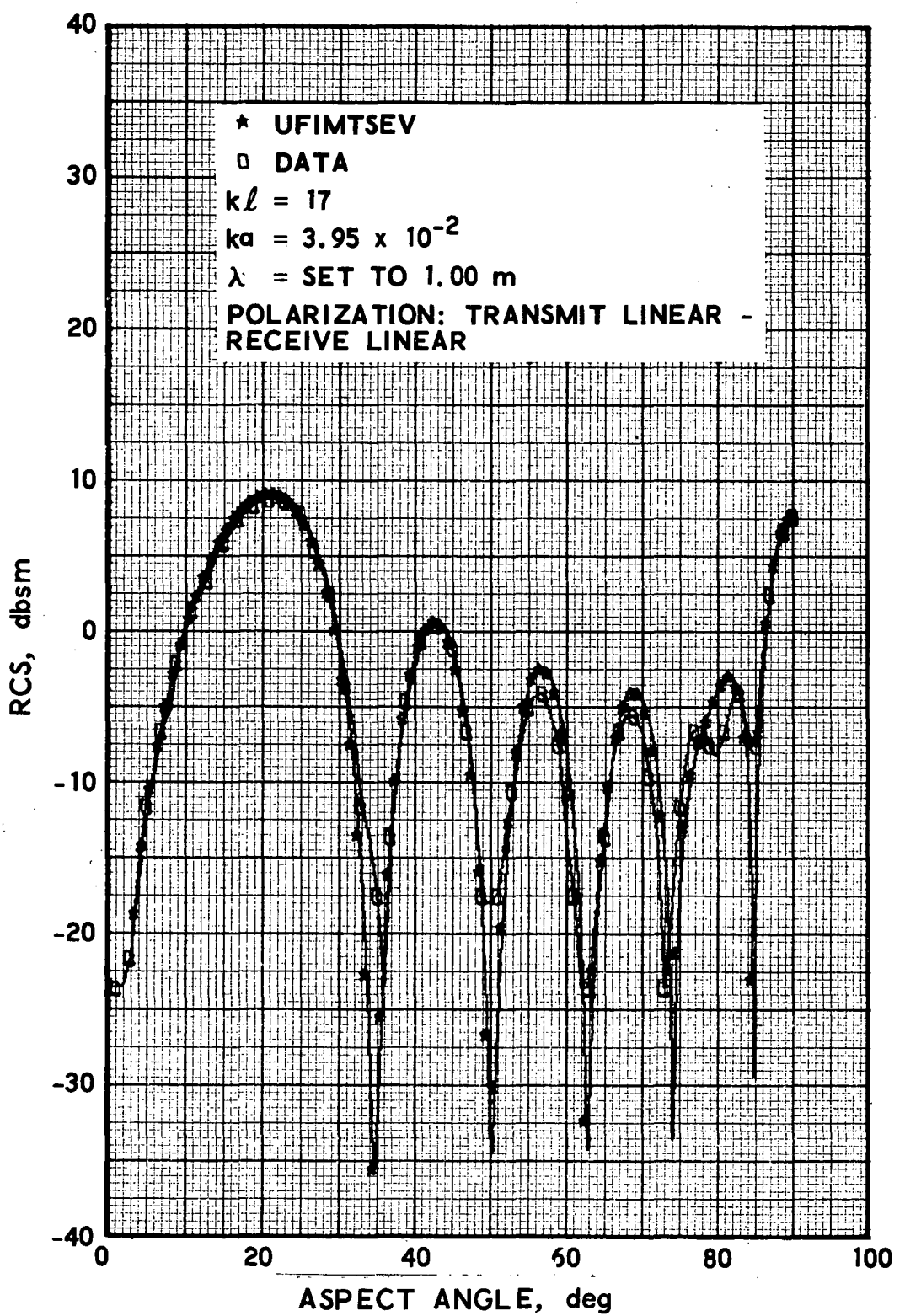


Figure 28. Comparison of Ufimtsev's Predicted RCS with Measured Data,  $k\ell = 17$

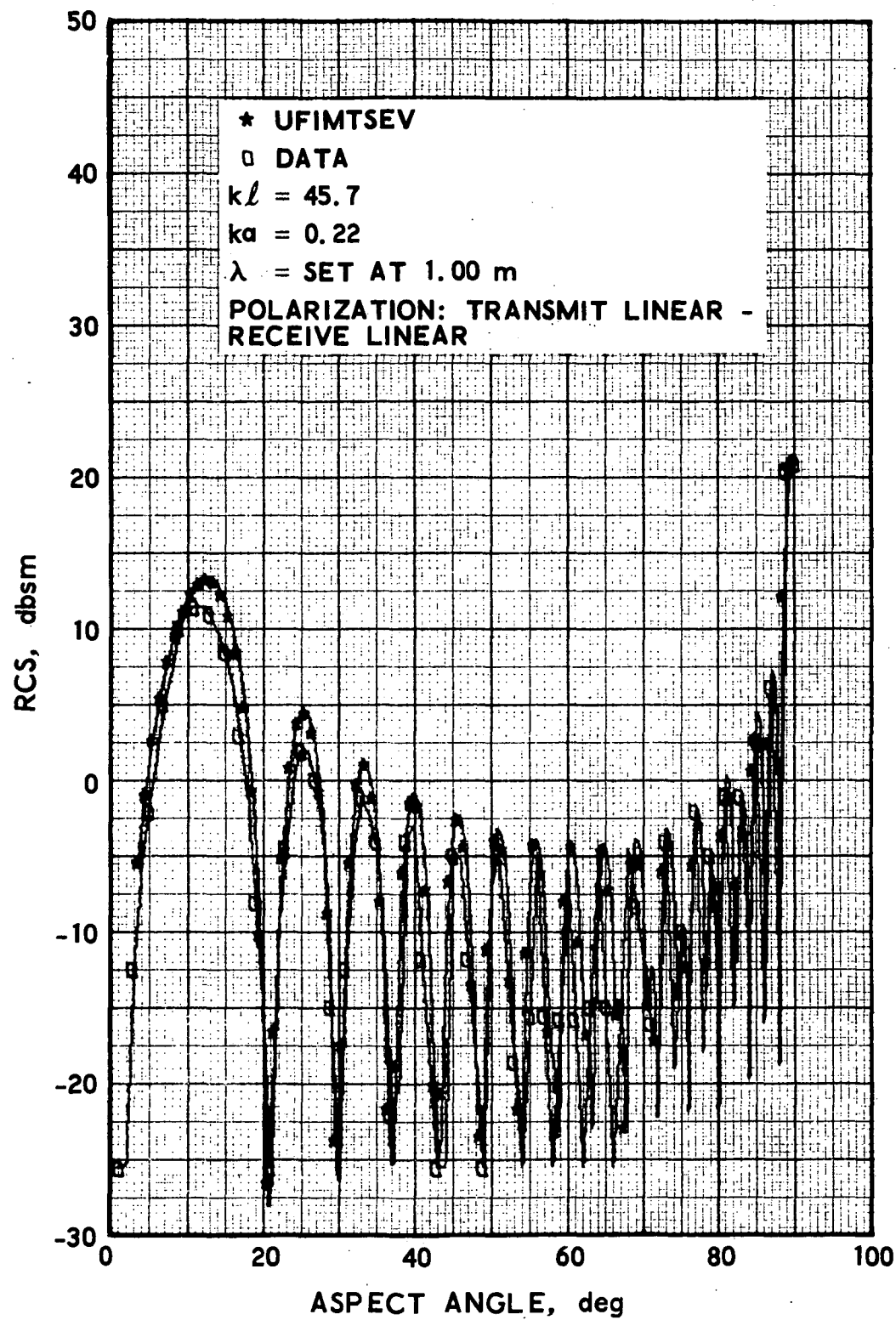


Figure 29. Comparison of Ufimtsev's Predicted RCS with Measured Data,  $k\ell = 45.7$

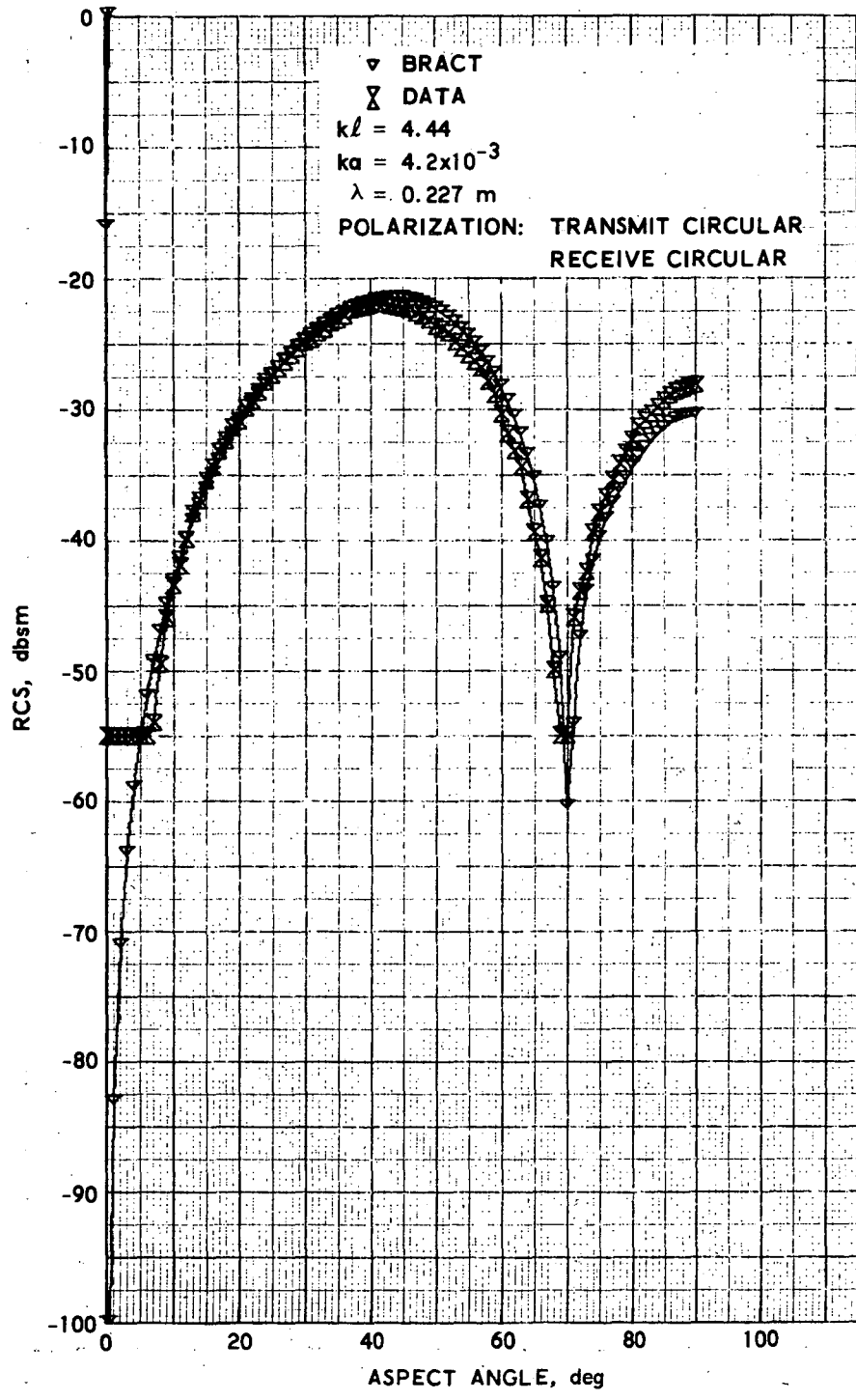


Figure 30. Comparison of BRACT Calculated RCS with Measured Data,  $k\bar{l} = 4.44$

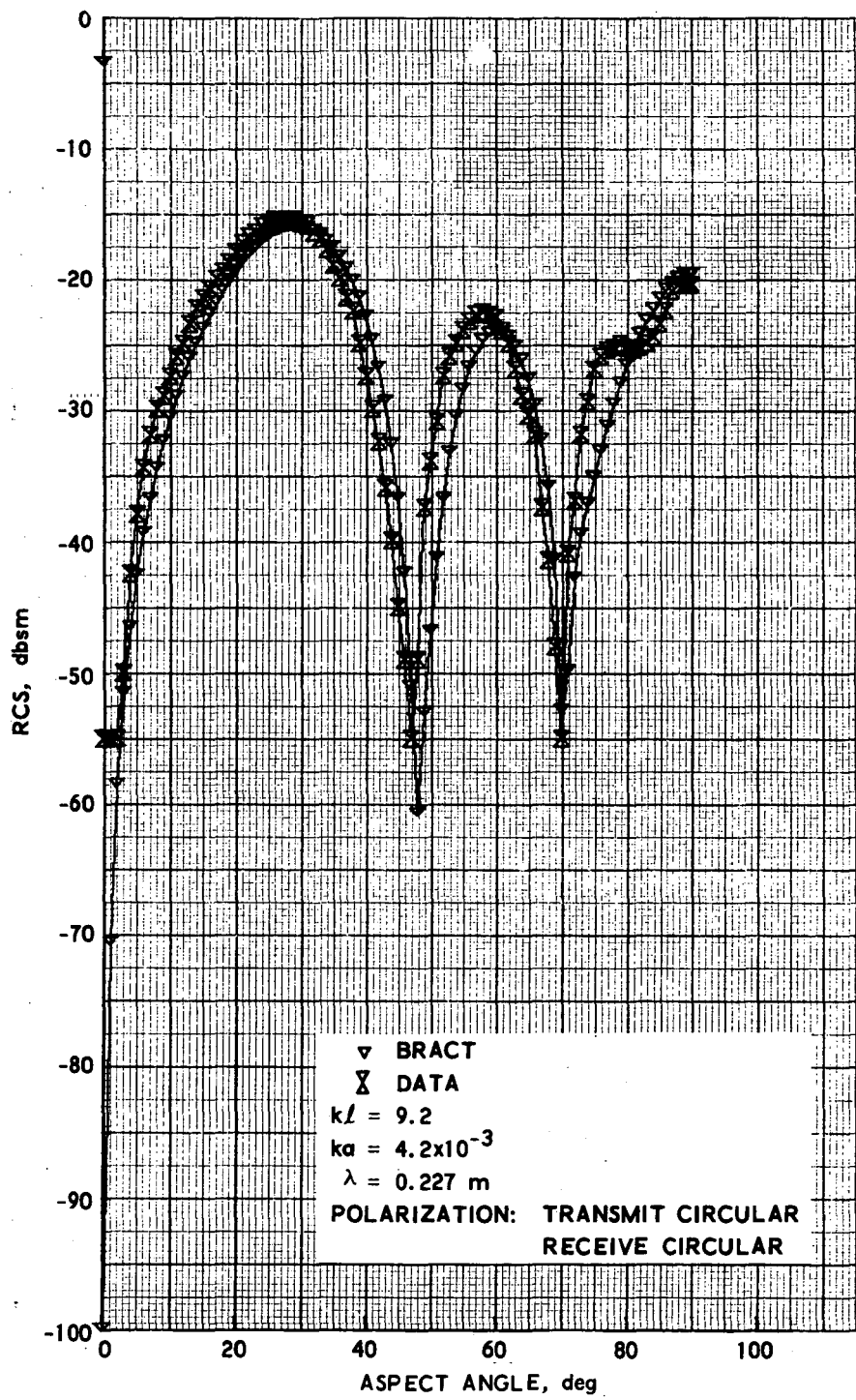


Figure 31. Comparison of BRACT Calculated RCS with Measured Data,  $kl = 9.2$

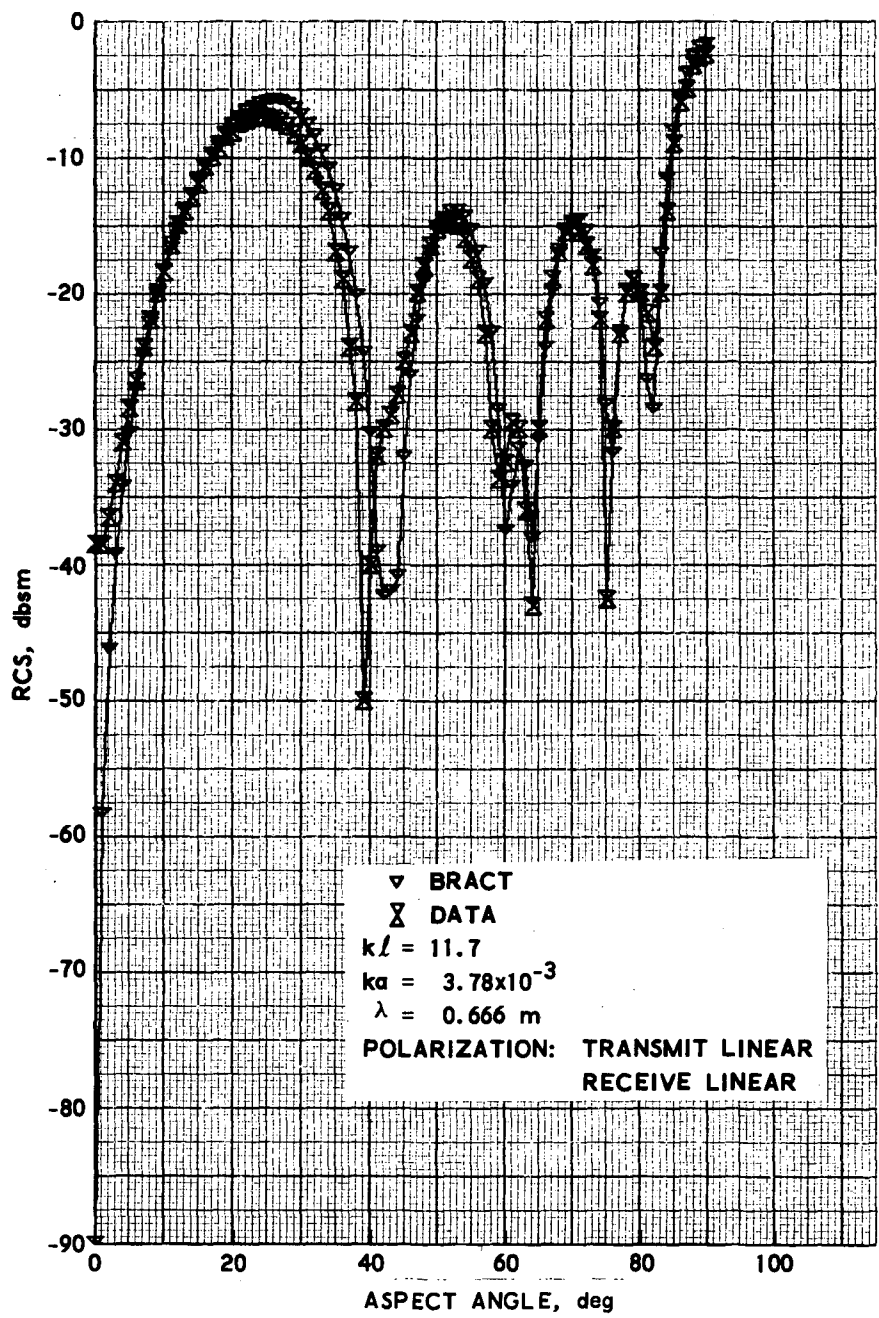


Figure 32. Comparison of BRACT Calculated RCS with Measured Data,  $k\ell = 11.7$

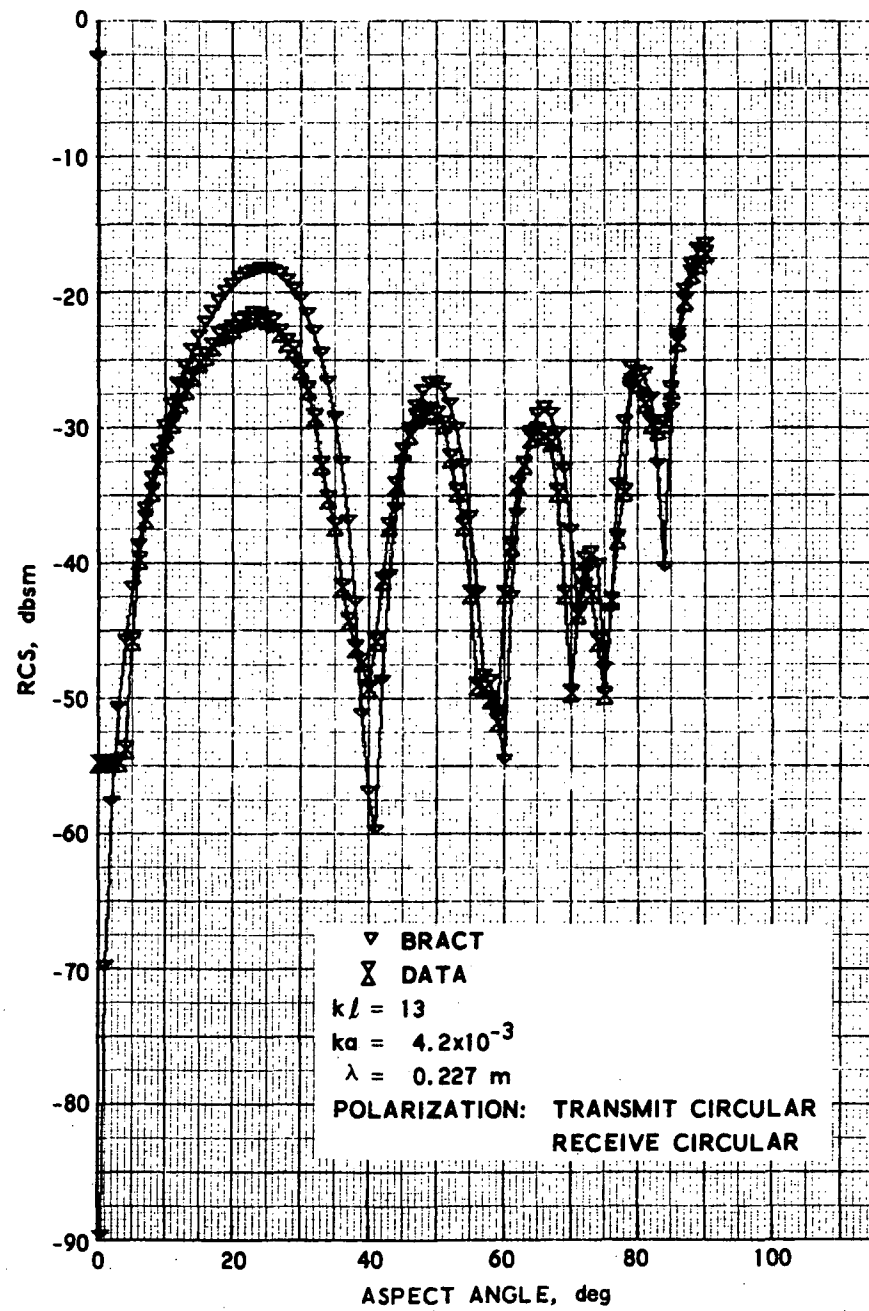


Figure 33. Comparison of BRACT Calculated RCS with Measured Data,  $k\ell = 13$

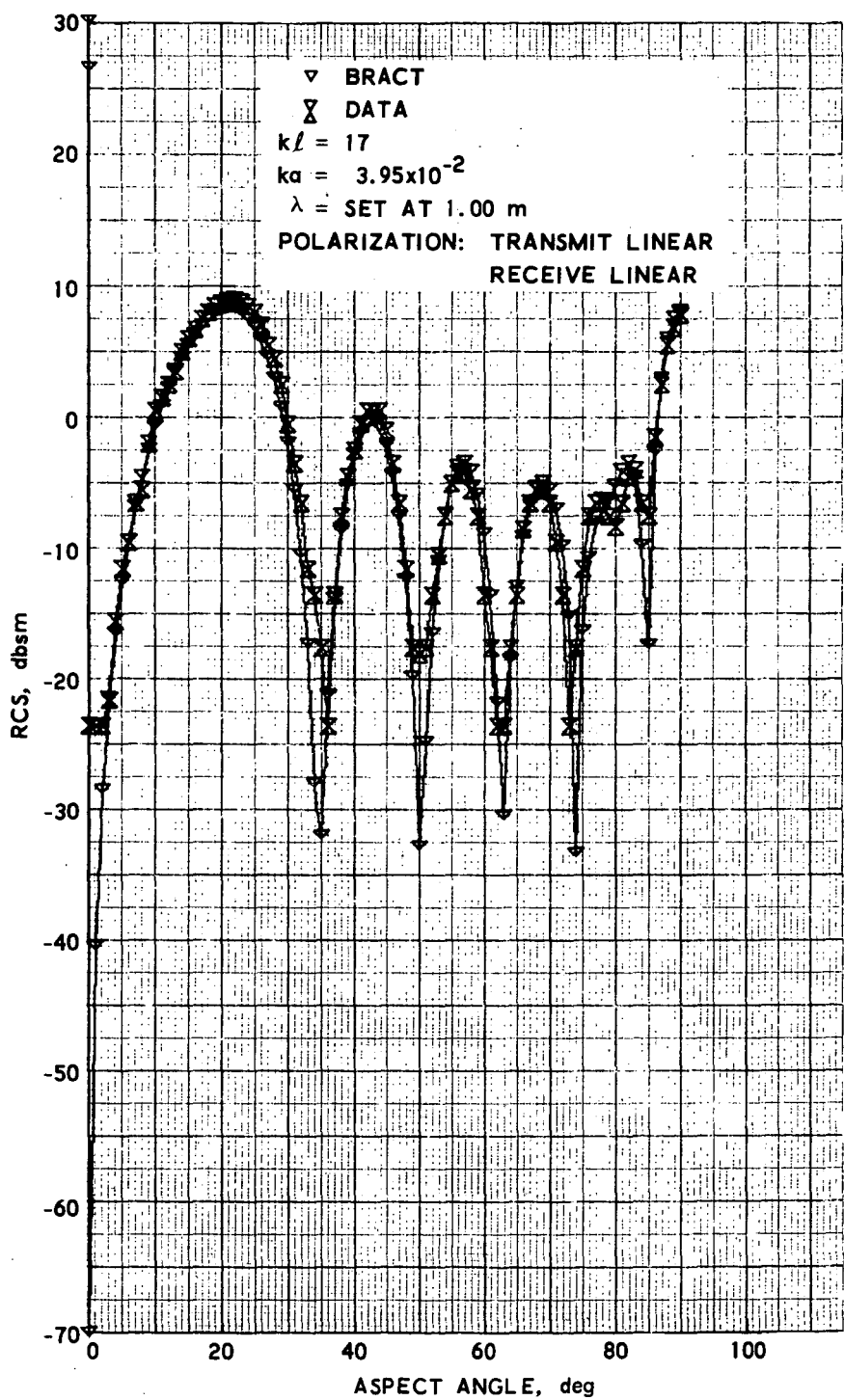


Figure 34. Comparison of BRACT Calculated RCS with Measured Data,  $k\ell = 17$

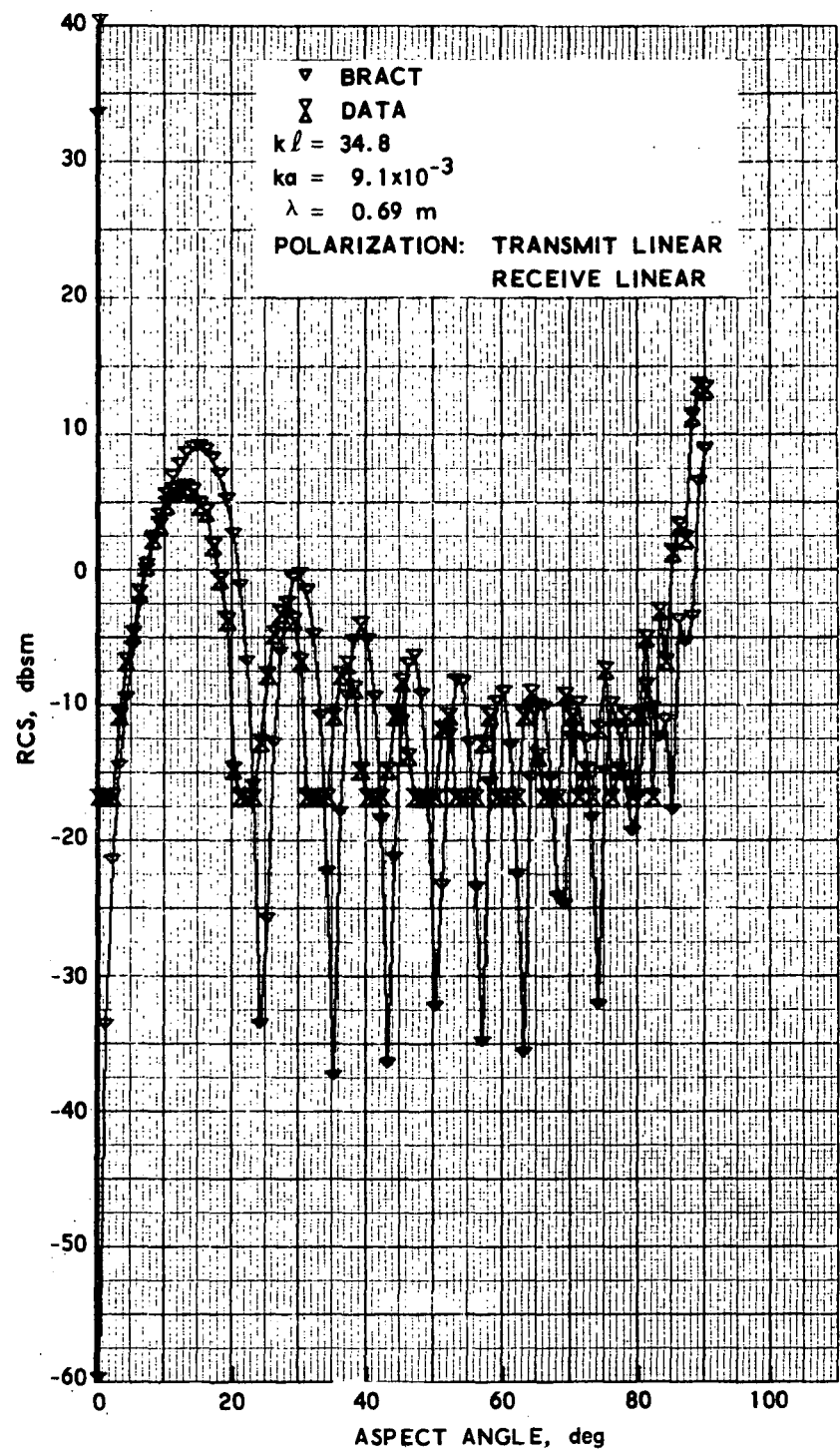


Figure 35. Comparison of BRACT Calculated RCS with Measured Data,  $k\ell = 34.8$

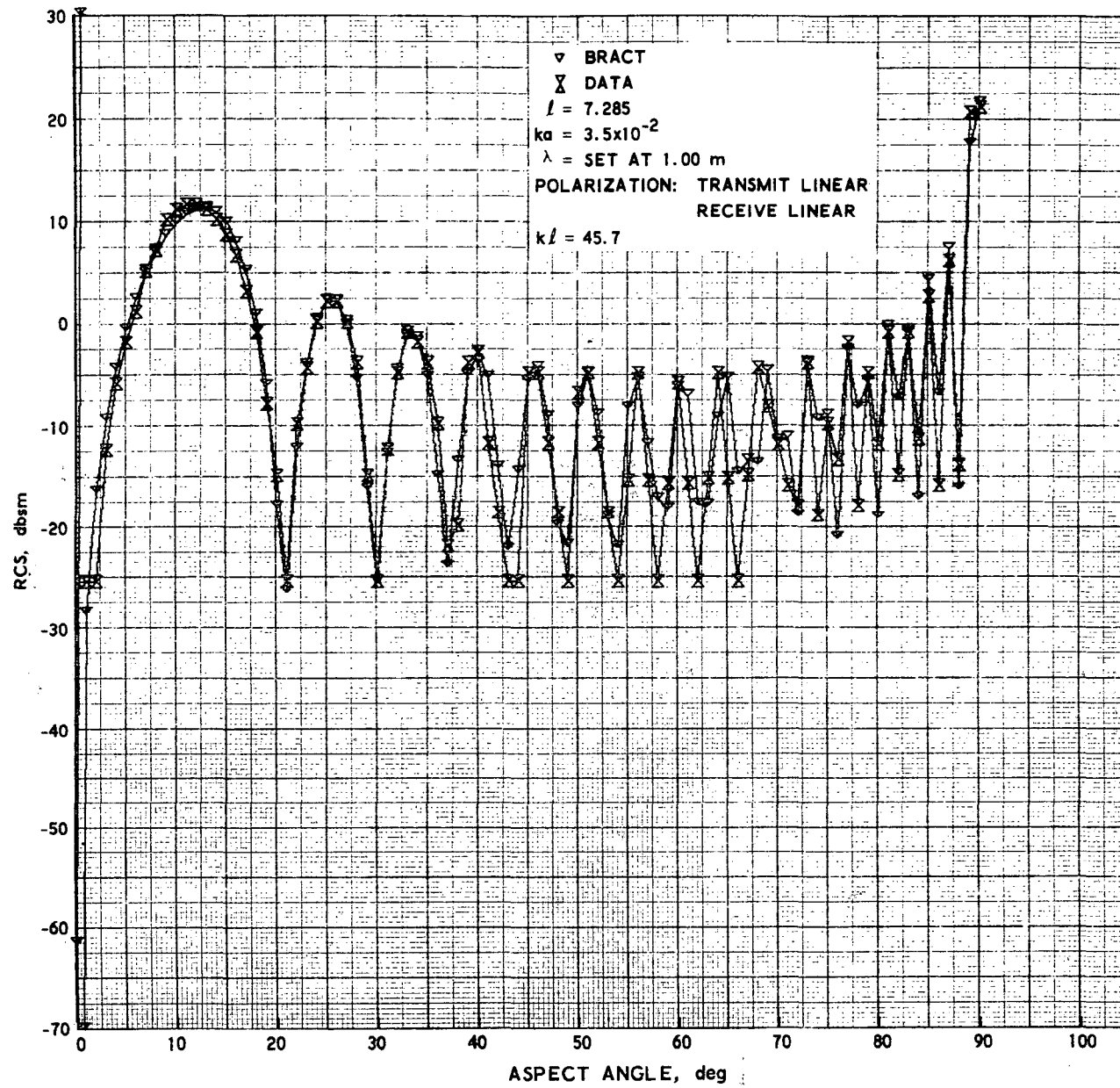


Figure 36. Comparison of BRACt Calculated RCS with Measured Data,  $kl = 45.7$

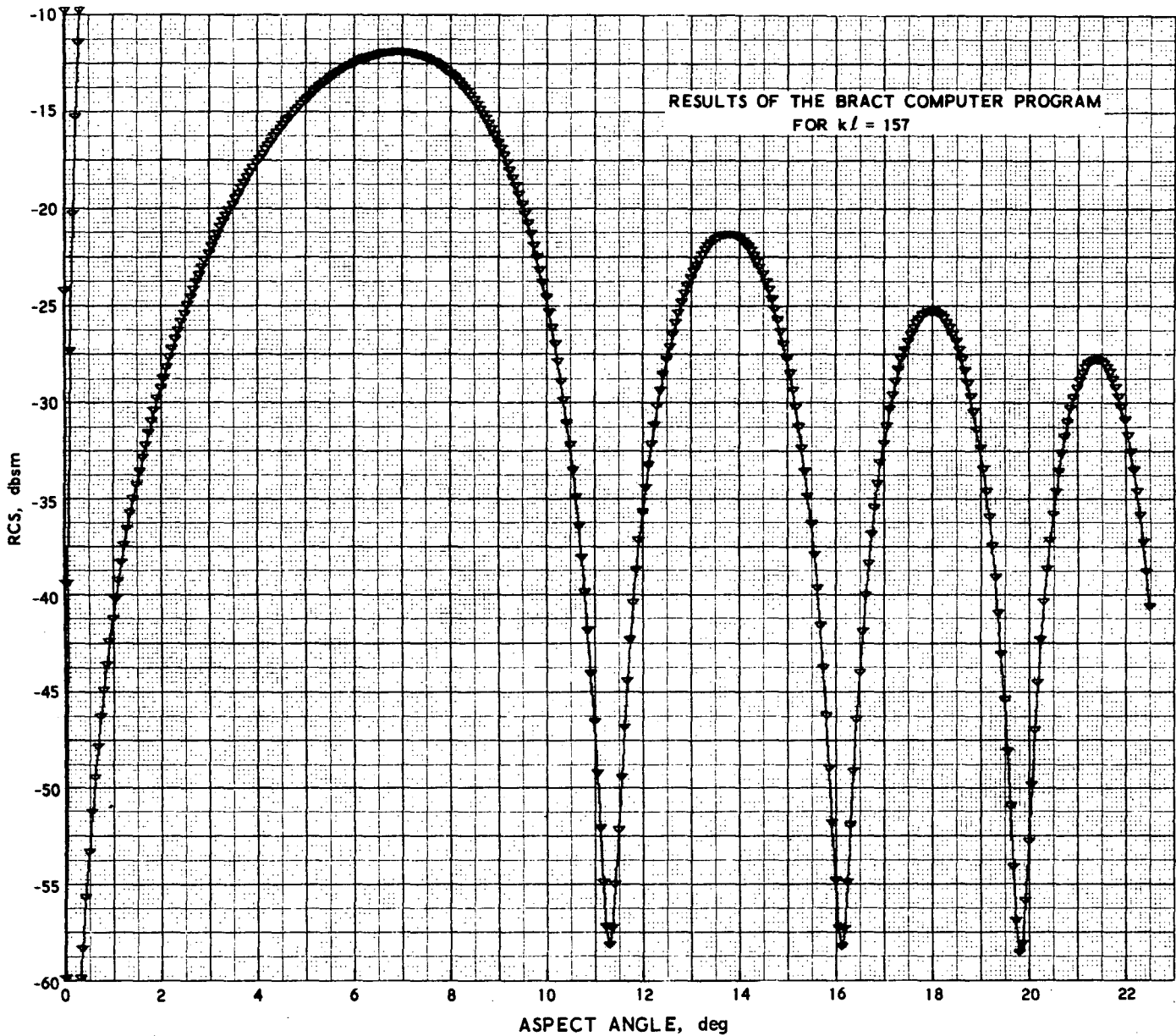


Figure 37a. BRACT Calculated RCS,  $k\ell = 157$  (Sheet 1)

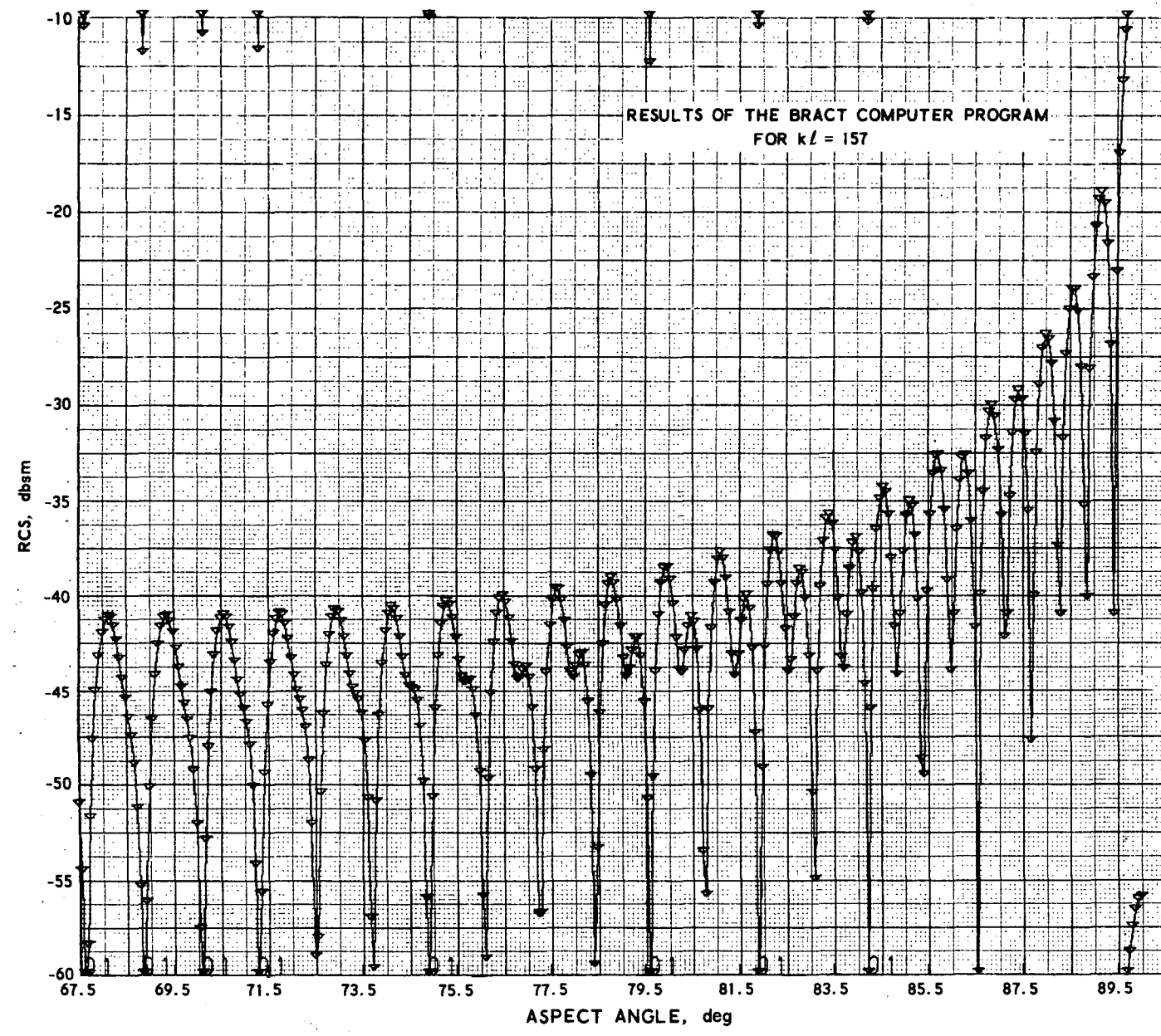


Figure 37b. BRACT Calculated RCS,  $k\ell = 157$  (Sheet 2)

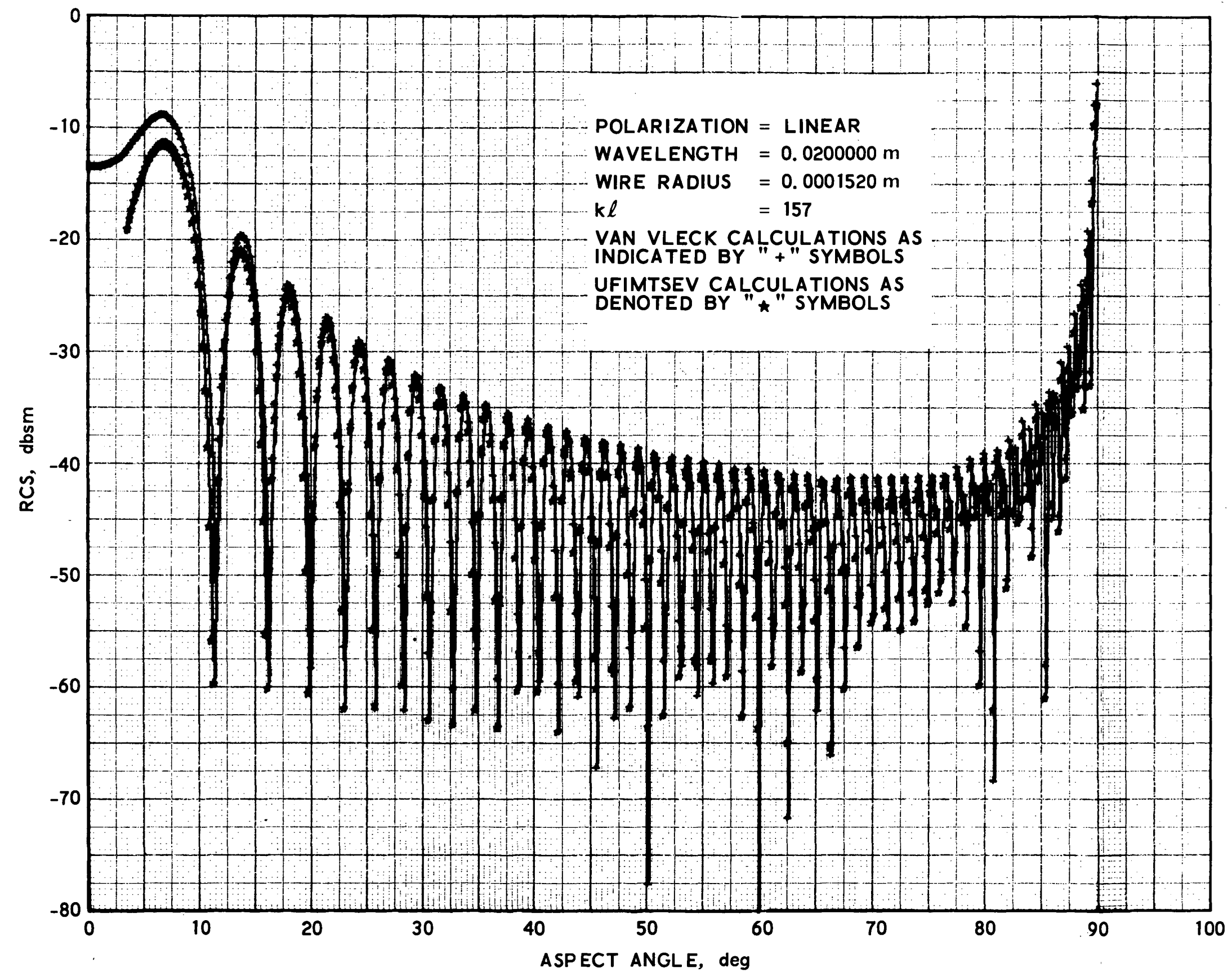


Figure 38. Van Vleck vs Ufimtsev Predicted RCS Values,  $k\ell = 157$

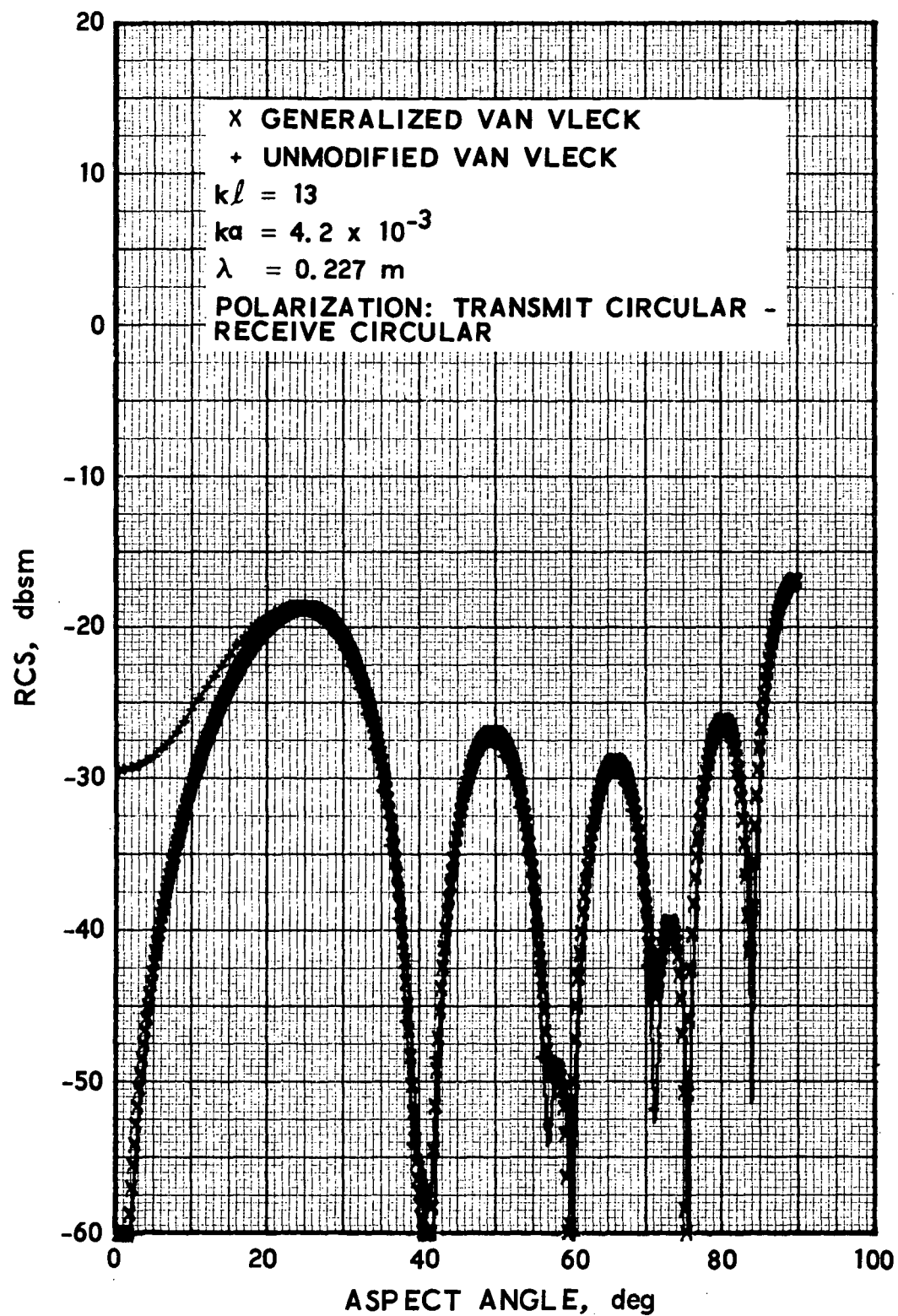


Figure 39. Comparison of the Generalized Van Vleck Formulation with Van Vleck's original Expression,  $k\ell = 13$

## APPENDIX A

The expressions for monostatic cross section from a generalized Van Vleck (Ref. 8) theory would be

$$\sigma(\theta) = \frac{\lambda^2 \cos^4 \phi}{\pi K K^*} E_1 E_1^* \quad (A-1)$$

$$E_1 = \frac{\sin 2q\ell}{\cos \theta} - (A + B) \frac{\sin (\beta + q)\ell}{1 + \cos \theta} - (A - B) \frac{\sin (\beta - q)\ell}{1 - \cos \theta} \quad (A-2)$$

$$q = \beta \cos \theta \quad (A-3)$$

$$\beta = \frac{2\pi}{\lambda} \quad (A-4)$$

$$A = \frac{2K \cos q\ell - (De^{iq\ell} + Ge^{-iq\ell})}{2L \cos \beta\ell - (Ee^{i\beta\ell} + Fe^{-i\beta\ell})} \quad (A-5)$$

$$B = \frac{2iK \sin q\ell - (De^{iq\ell} - Ge^{-iq\ell})}{2iL \sin \beta\ell - (Ee^{i\beta\ell} - Fe^{-i\beta\ell})} \quad (A-6)$$

$$F = C \sin 2\beta\ell \quad (A-7)$$

$$E = F - C \sin 4\beta\ell - iS \sin 4\beta\ell \quad (A-8)$$

$$G = F - C \sin 2(\beta - q)\ell - iS \sin 2(\beta - q)\ell \quad (A-9)$$

$$D = F - C \sin 2(\beta + q)\ell - iS \sin 2(\beta + q)\ell \quad (A-10)$$

$$L = 2 \log_2 \left( \frac{2\ell}{a} \right) + 2 \log 2 + \frac{a}{\ell} - \text{Cin } 4\beta\ell - \frac{\sin 4\beta\ell}{4\beta\ell} - 1$$

$$- i \left[ \text{Si} 4\beta\ell + \frac{(\cos 4\beta\ell - 1)}{4\beta\ell} \right] \quad (A-11)$$

$$K = 2 \log_2 \left( \frac{2\ell}{a} \right) + 2 \log 2 + \frac{a}{\ell} - \text{Cin } 2(\beta + q)\ell$$

$$- \text{Cin } 2(\beta - q)\ell - \frac{\sin 2(\beta + q)\ell}{2(\beta + q)\ell} - \frac{\sin 2(\beta - q)\ell}{2(\beta - q)\ell}$$

$$- i \left\{ \text{Si} 2(\beta + q)\ell + \text{Si} 2(\beta - q)\ell + \frac{[\cos 2(\beta + q)\ell - 1]}{2(\beta + q)\ell} \right.$$

$$\left. + \frac{[\cos 2(\beta - q)\ell - 1]}{2(\beta - q)\ell} \right\} \quad (A-12)$$

$$\text{Cin } x = \int_0^x \frac{1 - \cos y}{y} dy = - \sum_{n=1}^{\infty} \frac{(-1)^n x^{2n}}{2n(2n)!} \quad (A-13)$$

$$\text{Si } x = \int_0^x \frac{\sin y}{y} dy = \sum_{n=0}^{\infty} \frac{(-1)^n x^{2n+1}}{(2n+1)(2n+1)!} \quad (A-14)$$

$\ell$  = length of wire

$a$  = radius of wire

$\theta$  = angle between the propagation vector and the wire

$\phi$  = angle between the  $\vec{E}$  vector and the plane formed by the wire and the propagation vector.

## UNCLASSIFIED

Security Classification

## DOCUMENT CONTROL DATA - R &amp; D

(Security classification of title, body of abstract and indexing annotation must be entered when the overall report is classified)

1. ORIGINATING ACTIVITY (Corporate author)	2a. REPORT SECURITY CLASSIFICATION Unclassified
The Aerospace Corporation El Segundo, California	2b. GROUP

## 3. REPORT TITLE

PREDICTED RADAR CROSS SECTION OF THIN, LONG WIRES  
COMPARED WITH EXPERIMENTAL DATA

## 4. DESCRIPTIVE NOTES (Type of report and inclusive dates)

## 5. AUTHOR(S) (First name, middle initial, last name)

Jacques Renau and Michael T. Tavis

6. REPORT DATE 72 OCT 01	7a. TOTAL NO. OF PAGES 66	7b. NO. OF REFS 8
8a. CONTRACT OR GRANT NO. F04701-72-C-0073	9a. ORIGINATOR'S REPORT NUMBER(S) TR-0073(3450-16)-2	
b. PROJECT NO.		
c.	9b. OTHER REPORT NO(S) (Any other numbers that may be assigned this report) SAMSO- TR- 73-136	
d.		

## 10. DISTRIBUTION STATEMENT

Approved for public release; distribution unlimited

11. SUPPLEMENTARY NOTES	12. SPONSORING MILITARY ACTIVITY Space and Missile Systems Organization Air Force Systems Command Los Angeles, California
-------------------------	--

## 13. ABSTRACT

In order to determine the validity and accuracy of Radar Cross Section (RCS) predictions for thin wires, the predictions of the closed-form expressions developed by Chu, Tai, Van Vleck, et al., and Ufimtsev have been compared with carefully measured backscattered RCS vs angle of incidence for various length thin, long, cylindrical conductors. Further, the prediction of an open-form numerical analysis based on the Source Distribution Technique and programmed by M. B. Associates as the BRAC computer program was also compared with the experimental data.

It was found that (1) the BRAC computer results agree with experiment so well (within  $\pm 1$  dB for all reliable data) that it may be used with great confidence for any length thin wires and can be used as reference data for comparing with the prediction of the close-form solutions; (2) the results of Chu are not accurate except at broadside incidence; (3) the results of Tai compare favorably with data up to  $kL$  values of about 17 if corrections are made to the approximate formulas to correct for broadside incidence; (4) the results of Ufimtsev compare well with experiment for all  $kL$  values considered; and (5) the results of Van Vleck, et al., appear to be very accurate for all  $kL$  values considered except for near end-on incidence. In a separate report to be published soon one of the authors of this report (M. Tavis) has shown that this deficiency is due to numerical approximations in the theoretical expressions.

**UNCLASSIFIED**

Security Classification

14.

**KEY WORDS**

RCS of Thin Wires

Analytical Expressions of RCS of Wires

Wire RCS

Computer Predictions of RCS

Comparison of RCS Predictions

Distribution Statement (Continued)

Abstract (Continued)

**UNCLASSIFIED**

Security Classification